JAERI-M
88-062

JAPANESE CONTRIBUTIONS TO IAEA INTOR WORKSHOP PHASE TWO A, PART 3

CHAPTER XI : SYSTEM ANALYSIS OF INTOR-LIKE DESIGNS

March 1988

Tadanori MIZOGUCHI[*1], Hiromasa IIDA, Masayoshi SUGIHARA
Noboru FUJISAWA, Tsutomu HONDA[*2], Takeshi KOBAYASHI
Nobuharu MIKI, Kunihiko NAKASHIMA, Satoshi NISHIO
Ryusei SAITO and Masao YAMADA

日 本 原 子 力 研 究 所
Japan Atomic Energy Research Institute

JAERI-Mレポートは，日本原子力研究所が不定期に公刊している研究報告書です。
入手の問合わせは，日本原子力研究所技術情報部情報資料課（〒319－11茨城県那珂郡東海村）あて，お申しこしください。なお，このほかに財団法人原子力弘済会資料センター（〒319-11茨城県那珂郡東海村日本原子力研究所内）で複写による実費頒布をおこなっております。

JAERI-M reports are issued irregularly.
Inquiries about availability of the reports should be addressed to Information Division, Department of Technical Information, Japan Atomic Energy Research Institute, Tokai-mura, Naka-gun, Ibaraki-ken 319-11, Japan.

編集兼発行　日本原子力研究所
印　　刷　日立高速印刷株式会社

Japanese Contributions to IAEA INTOR Workshop Phase Two A, Part 3 Chapter XI: System Analysis of INTOR-like Designs

Tadanori MIZOGUCHI,[*1] Hiromasa IIDA, Masayoshi SUGIHARA
Noboru FUJISAWA, Tsutomu HONDA,[*2] Takeshi KOBAYASHI
Nobuharu MIKI, Kunihiko NAKASHIMA, Satoshi NISHIO
Ryusei SAITO and Masao YAMADA

Department of Large Tokamak Research
Naka Fusion Research Establishment
Japan Atomic Energy Research Institute
Naka-machi, Naka-gun, Ibaraki-ken

(Received February 8, 1988)

This report corresponds to Chapter XI of Japanese contribution report to IAEA workshop, Phase Two A, Part 3. The purpose of this system analysis is to clarify the reason why the INTOR-like designs of each delegation differ from each other. Benchmark studies of INTOR (IAEA), FER (Japan), NET (EC) TIBER (USA) and OTR (USSR) are carried out by the conceptual design system code (TRESCODE). As results of the global sensitivity analysis, it is found that the choices of design features/drivers give the largest impact on the reactor size and capital cost. There is smooth correlation between plasma major radius and capital cost. Individual sensitivity analysis reveals that additional ignition margin, higher Z_{eff}, higher toroidal field coil design and change of operation scenario (hybrid to full inductive) result in an increase of reactor size and cost.

Keyrords: INTOR, Phase Two A Part 3, IAEA System Analysis, INTOR-like Designs

---

*1 On leave from Hitachi, Ltd.

*2 Toshiba Cooporation

IAEA INTOR ワークショップフェーズ IIA パート3 報告書
第11章：INTOR相応次期装置のシステム解析

日本原子力研究所那珂研究所臨界プラズマ研究部
溝口 忠憲[*1]・飯田 浩正・杉原 正芳・藤沢 登
本多 力[*2]・小林 武司・三木 信晴・中島 国彦
西尾 敏・斉藤 龍生・山田 政男

（1988年2月8日受理）

本報告書はIAEA主催INTORワークショップフェーズIIA，パート3の日本報告書，第11章INTOR相応次期装置設計のシステム解析，に相応する。システム解析の主なる目的は，INTORと同様の考え方にたつ各国の次期装置が，設計段階で何故ちがいが生じるのかを明確にすることである。概念設計システムコード（TRESCODE）を用いて，INTOR（IAEA），FER（日本）NET（EC），TIBER（米国），OTR（ソ連）のベンチマーク計算を実施した。その過程で，プラズマ条件，工学設計条件の相異及びそのインパクトを把握した。炉サイズ及びコストに最も大きなインパクトを与えるのはミッションの選定，設計ドライバーの選択にあることが明らかになった。またイグニションマージン，Z_{eff}トロイダル磁場，供給磁束などの設計パラメーターがサイズ増大，コスト高に非常に敏感であるとが明らかにされた。

那珂研究所：〒311-01 茨城県那珂郡那珂町大字向山801-1
*1 外来研究員 日立製作所㈱
*2 ㈱東芝

Contents

目　　次

1. Introduction

The critical analysis of INTOR-like designs was implemented as a home task of engineering group at the session XIV session in December 1986. The purpose of this analysis is to clarify the reasons why the INTOR-like designs differ from each other. The results of this analysis is expected to give useful data base for discussing ITER design concept.

Some of the necessary input for this analysis was discussed and prepared at the Specialist Meeting on the next generation device last March. However, the information about the design methods emplayed by other parties, which is essential for this analysis, has not been obtained enough. Nevertheless, we conducted comparative studies between INTOR and FER and between NET and FER. Preliminary results of the analysis is described here.

At the session XIV the analytic procedure was defined as a global comparison of each country's INTOR-like design. Then later at the session XV, sensitivity analysis by changing single design option, for example shield thickness, was added. The later process has been done based on the own national INTOR-like design.

2. Description of Systems Analysis Codes

The tokamak reactor system conceptual design code (TRESCODE) has been developed at JAERI on the basis of FER design studies.[1] There are two objects for developing the design code. The first object is that TRESCODE can be applicable to the scoping studies for various reactor concepts. In this objects, relative cost estimations in terms of volume/weight and input/output energy can be carried out under the design driver/constraints of physics and engineering. Cost effective reactor concept is to be selected in this process, while optimization will be desired for further studies. The second object is that TRESOCDE can be used for engineering design of tokamak core structure for the selected reactor concept. In this objects, accurate radial-build and vertical-build based on shield calculation and stress/strain analysis of magnet system can be carried out under the design constraints/conditions. Operation scenario is included with plasma equilibrium and poloidal field calculations to obtain the final results.

The code consists of six major blocks namely plasma power balance calculation with core structure restriction, toroidal field coil design, poloidal field coils design with plasma equilibrium and field calculations, operation scenario, electric power supply analysis and relative cost estimation. Basic flow chart is shown in Fig. 2.1. In the process of determining inner torus radial build, shield requirements given as constraints for neutron wall load and liftime fluence are solved consistently by introducing a simplified shield calculation model. The radius of solenoid coils is also solved consistently under necessary volt second resulted from burn time and operation scenario as design driver in physics. The current density of TFC's conductor is principally determined by B-J_C relation. TFC case is designed to satisfy allowable stress intensity for primary membrane stress agsinst in-plane and over-turning force at all. Poloidal field coils positions are automatically determined with reflecting prohibition regions such as access port, torus core supporting leg, et. al.. PFC cross section and their final positions are solved consistantely with conductor design constraints and operation scenario. Operation scenario is one of important design driver to determine not only reactor size but also reactor's capability. In this code, however, one aspect of operation scenario, that is, a required volt

second is discussed in detail. Reactor size and PFC system strongly depends on this considerations. The electric power supply is also estimated consistently with the operations secenario. The accumulated capacity of the PFC power supplies will be dominant to compare with that of TFC power supplies. Our main considerations in this code is appropriate evaluation of the PFC power supplies. In addition, the power supplies for heating and current driving is also discussed. Finally, cost estimation in terms of weight and energy is provided.

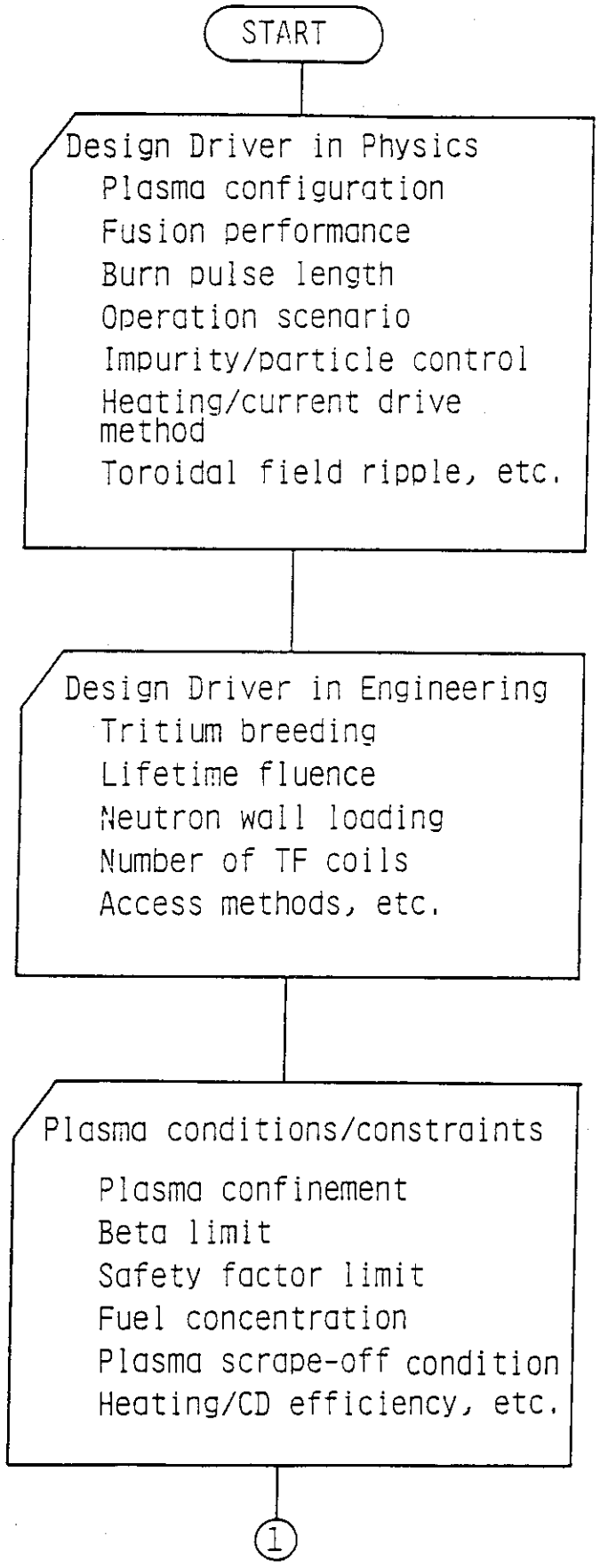

Fig. 2.1 Flow chart of TRESCODE

(Tokamak REactor System COnceptual DEsign code)

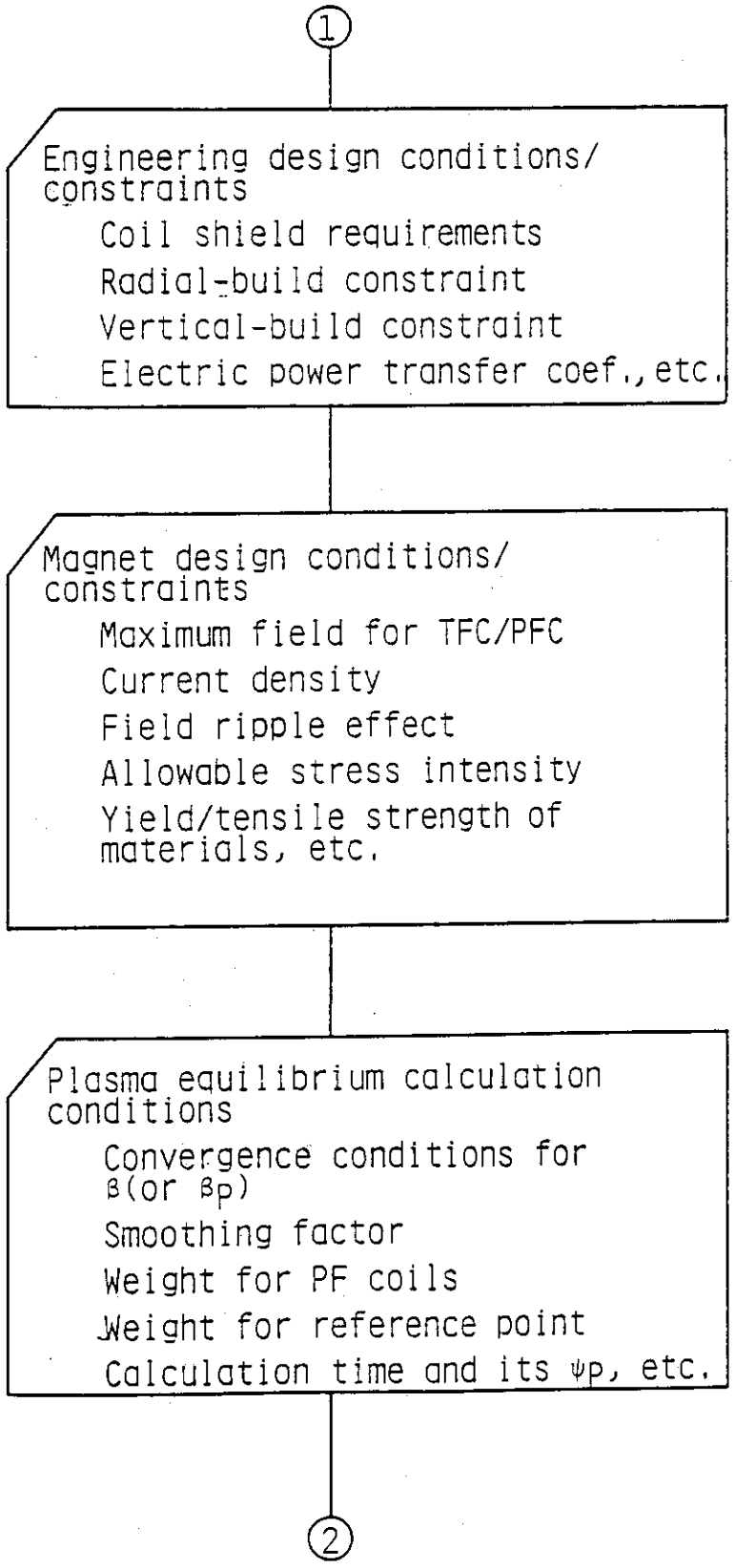

Fig. 2.1 (Continued)

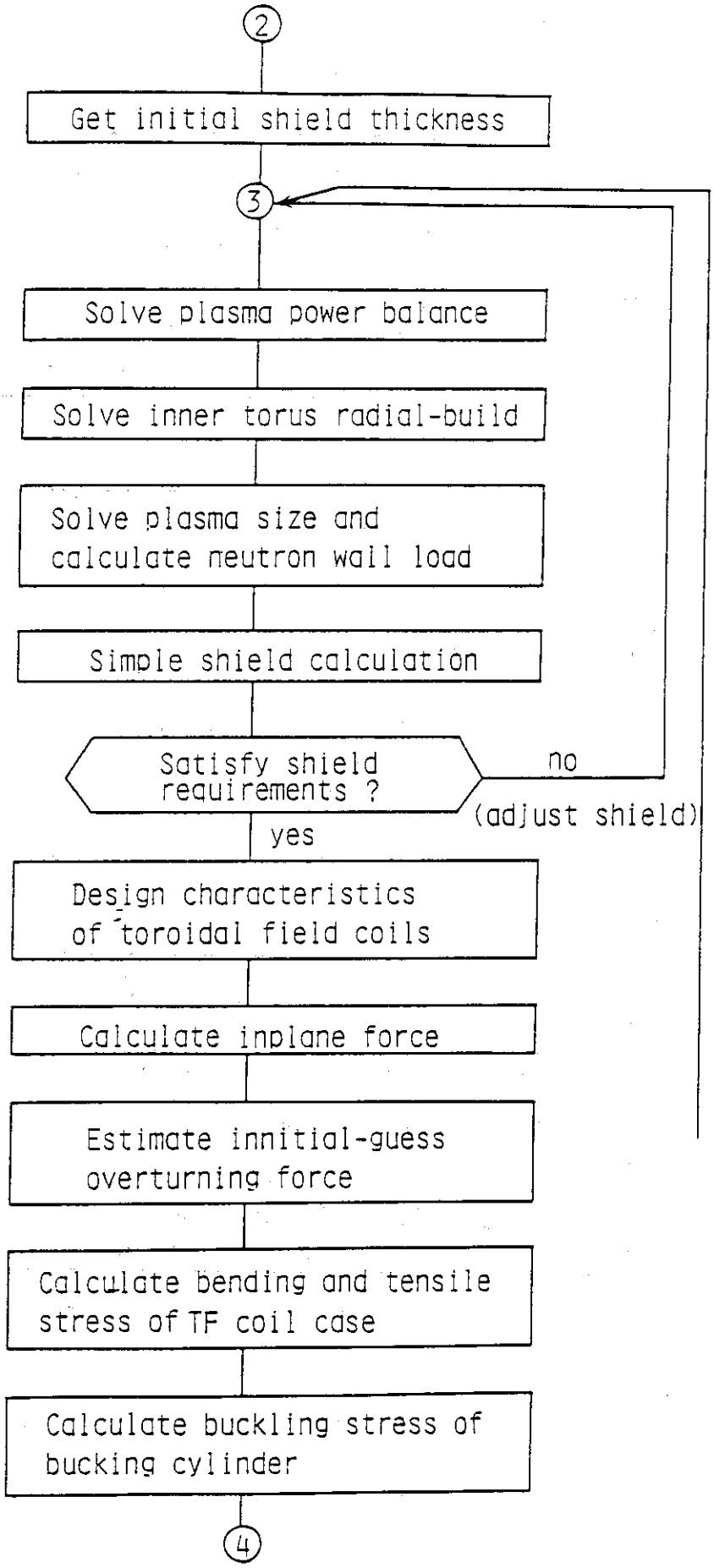

Fig. 2.1 (Continued)

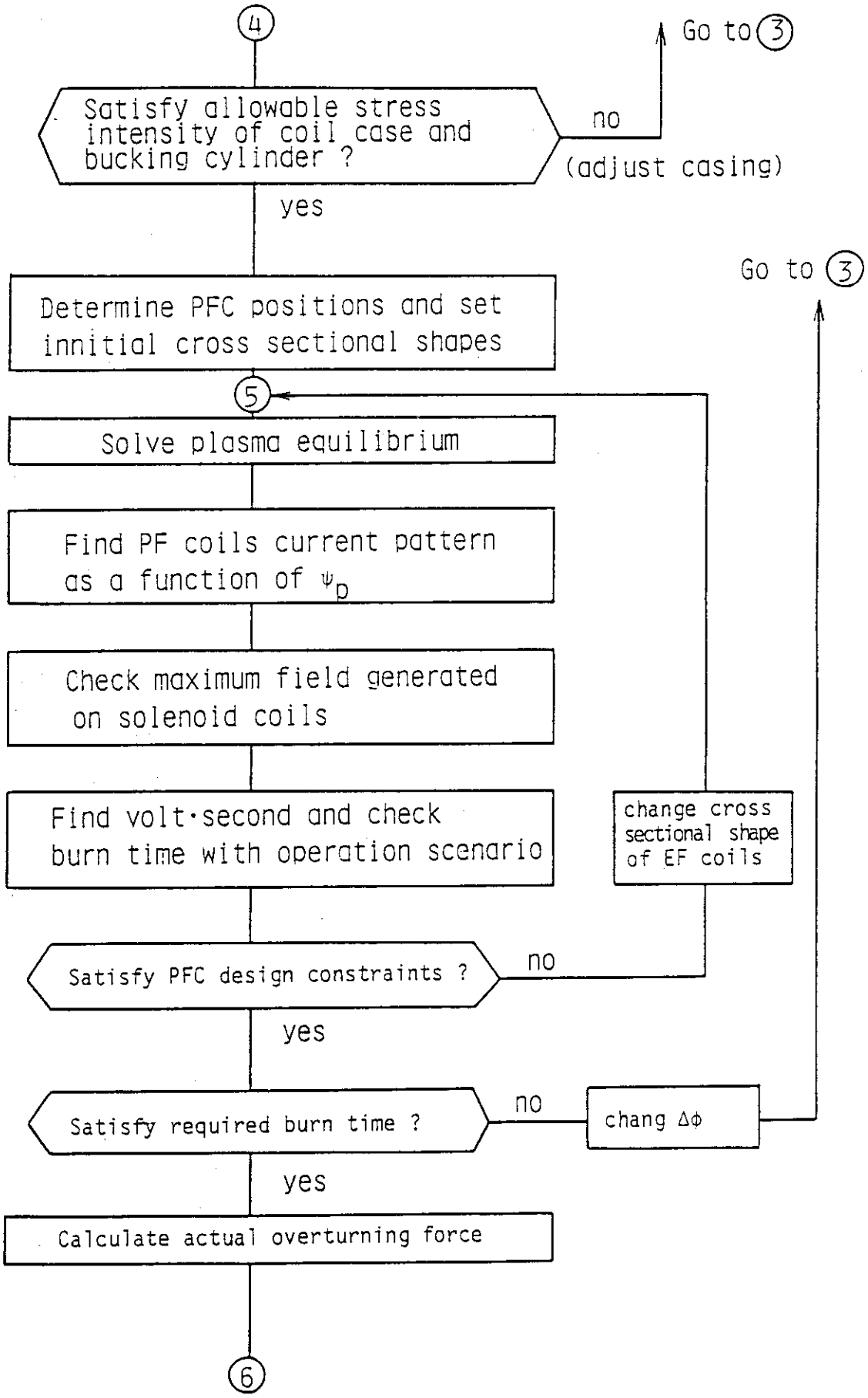

Fig. 2.1 (Continued)

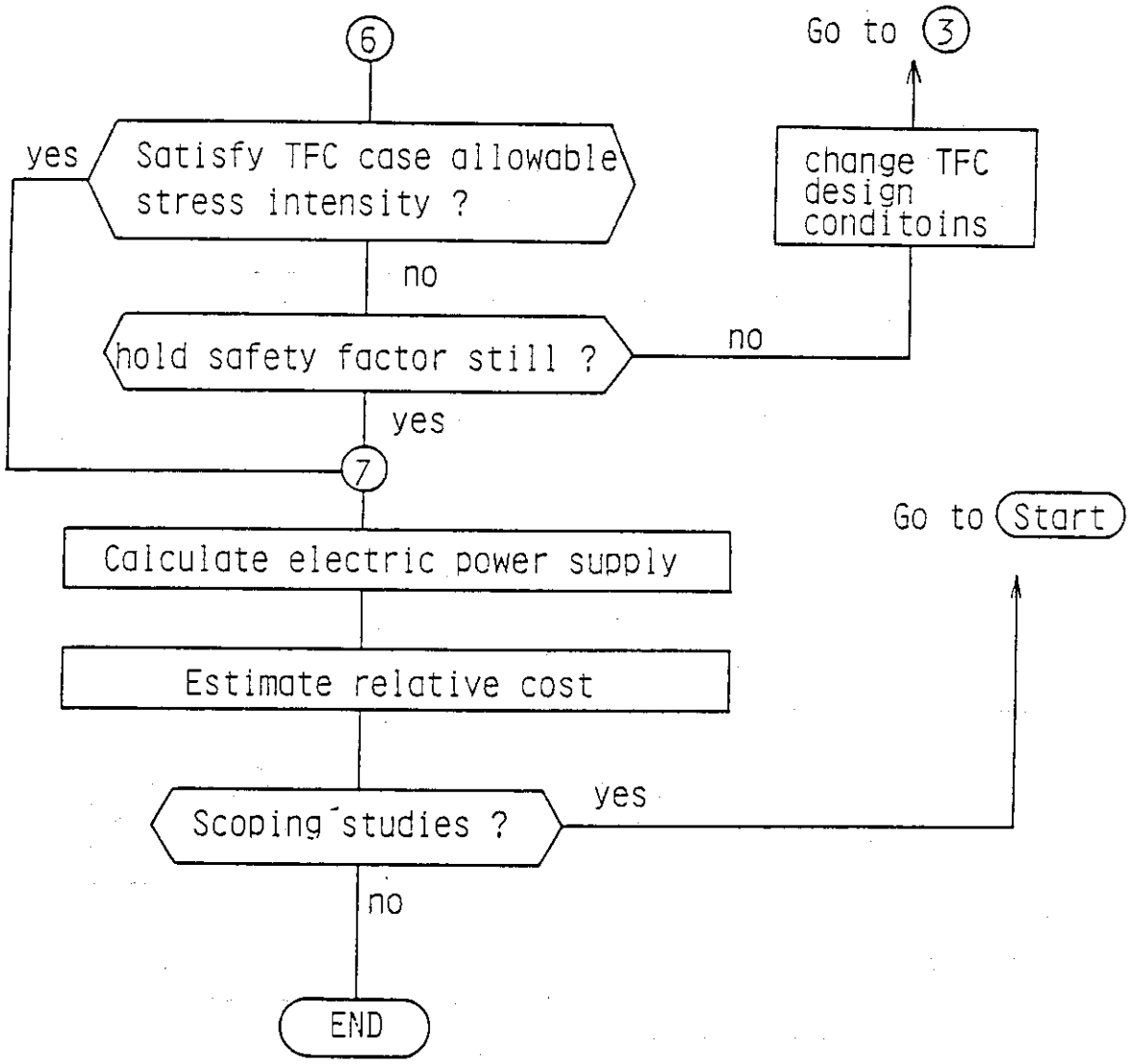

Fig. 2.1 (Continued)

3. Representation of INTOR-like Designs

3.1 Comparison of physics assumption

Each deligation has its own systems analysis code in order to optimize reactor design. In these calculational code many assumptions have been made to model plasma characteristics and components engineering designs and differe between countries. Table 3.1 summarizes the physics assumptions used each country.[2] One of the most significant difference is in the power balance considertion. FER takes radiation loss into account as energy loss term while INTOR, NET and OTR neglect it. For energy confinement various scaling laws are used. However all deligation except TIBER employs H mode type scalings.

Troyon scaling is employed by every deligation for the beta limit with a little different coeffficient. For Z_{eff} the difference is small except those employed by NET design. the ratio of total beta and fuel beta differs from 1.6 in TIBER to 1.2 in INTOR. The difference comes from the choise of Z_{eff} and fast α pressure contribution which largely depends on plasma temperature. For safety factor differes in two aspects, namely defined magnetic surface and plasma model (cylinder or tours). INTOR, OTR employs cylinder model, FER TIBER torus model and defined on 95% ψ_p and NET torus model and defined on the separatrix. There is some confusion between plasma specifications and the Physics in INTOR design. For example, the ratio of β and β_{DT} should be 1.19 according to the specifications, but 1.28 (at 10 keV) in the Physics constraints. The elongation of 1.6 described at both specifications and Physics is not the averaged elongation but the elongation at the non-null point side (or upper side) according to a plasma configuration figure. The averaged elongation should be about 1.75 on the surface defined by 95% of ψ_p.

Table 3.1 Comparison of NET, INTOR, FER, TIBER and OTR physics

Items	NET	FER	INTOR	TIBER	OTR
Power balance (for self-ignition)	$\frac{3\,k n_{DT} T}{\tau_E} = \frac{1.5\times10^6\,\beta_{DT}^2 B_T^4}{I_g}\frac{E_\alpha}{E_f}$ $I_g \equiv \frac{P_\alpha}{P_{loss}}$ $P_{loss} = \frac{3\,k n_{DT} T}{\tau_E}$	$\frac{\frac{3}{2}k(n_e+n_i)T}{\tau_E} + P_{br} + P_{sy}$ $= f_T\, n_D n_T \langle\sigma v\rangle E_\alpha(1+\frac{5}{Q})$ $f_T = 1.5$ $Q \geq 20$	$\frac{3\,k n_{DT} T}{\tau_E} = \frac{1.5\times10^6\,\beta_{DT}^2 B_T^4}{I_g}\frac{E_\alpha}{E_f}$ $I_g \equiv \frac{P_\alpha}{P_{loss}}$ $P_{loss} = \frac{3\,k n_{DT} T}{\tau_E}$	$\frac{\frac{3}{2}k(n_e T_e + n_i T_i)}{\tau_E}$ $=1.5\, n_D n_T \langle\sigma v\rangle E_\alpha(1+\frac{5}{Q})$ $Q \geq 5$	
Confinement time scaling law	ASDEX-H $\tau_E^{NET} = 0.065\, R_{(m)}\, I_{p(MA)} \sqrt{M}$ $M = 2.5$ with $I_g^{NET} = 2.9$	Mirnov-type $\tau_E^{FER} = 0.155\, a_{(m)}\, I_{p(MA)} \sqrt{\kappa}$	ASDEX-H $\tau_E = 0.12\, R_{(m)}\, I_{p(MA)}$ $I_g \sim 3.0$	Kaye-Goldston [4] $\tau_E = H \times \tau_E^{KG}$	T-11 [4]
Beta scaling law	Troyon scaling $\beta(\%) = G\,\frac{I_p(MA)}{a(m)\,B_T(T)}$ $G = 3.5$	Troyon scaling $\beta(\%) = G\,\frac{I_p(MA)}{a(m)\,B_T(T)}$ $G = 3.5$	Troyon scaling $\beta(\%) = G\,\frac{I_p(MA)}{a(m)\,B_T(m)}$ $G \sim 4.0$	Troyon scaling $\beta(\%) = G\,\frac{I_p(MA)}{a(m)\,B_T(m)}$ $G \sim 3.0$ or Yamazaki scaling	Troyon scaling $\beta(\%) = G\,\frac{I_p(MA)}{a(m)\,B_T(m)}$ $G = 3.5$

Table 3.1 (Continued)

Items	NET	FER	INTOR	TIBER	OTR
Ion composition	n_{He} = 8% + (i) n_{imp} (C,O) = 2% (ii) n_{imp} (medium Z) = 0.05% (iii) n_{imp} (high Z) = 0.005% Remains are $n_D + n_T$ ⇓ Z_{eff} = 2.0, n_e/n_{DT} = 1.34	n_{He} = 5% + $n_C = n_O$ = 0.5% n_H = 1% $n_D = n_T$ = 46.5% ⇓ Z_{eff} = 1.5, n_e/n_{DT} = 1.23	n_{ne} = 5% $n_C = n_O$ = 0.5% $n_D = n_T$ = 47% ⇓ Z_{eff} = 1.5	n_{He} = 5% n_O = 0.24% $n_D = n_T$ = 47.38% ⇓ Z_{eff} = 1.5	n_{He} = 5% n_H = 1% $n_c + n_O$ ~ 1% $n_D = n_T$ = 46.5% ⇓ Z_{eff} = 1.5
Fuel beta	β / β_{DT} = 1.34 fast α pressure = 10%	β / β_{DT} = 1.23 fast α pressure = 8% at 12 keV (5% at 10 keV)	β / β_{DT} = 1.19 fast α = 7 % at 10 keV	β / β_{DT} = 1.6 fast α pressure ?	β / β_{DT} = 1.2
Safety factor	$q_I = \frac{5a^2 B_T}{R\, I_p(MA)} K^2$ $K = \oint \frac{dl_p}{2\pi a}$ Surface for line integration: $R = R_p + a\cos(\theta + \delta_N \sin)$ $Z = \kappa_N a \sin\theta$ κ_N, δ_N are the noncircularity at the separatrix.	$q_\psi = \frac{5a^2 B_T}{R\, I_p(MA)} f(\kappa,\delta)$ $f(\kappa,\delta) = \frac{1+\kappa^2}{2}\left(1 + \frac{0.16+0.633\delta}{\sqrt{A}}\right) \times \left(1 + \frac{\beta_p(0.45+\delta)}{A^{1.5}}\right)$ κ, δ are the noncircularity at the surface defined by 95% ψ_p.	$q_I = \frac{5a^2 B_T}{R\, I_p(MA)} \frac{1+\kappa^2}{2}$ κ is the plasma average elongation at the surface defined by 95% ψ_p.	$q_I = \frac{5a^2 B_T}{R\, I_p(MA)} \frac{1+\kappa^2}{2}$ κ is the plasma average elongation at the surface defined by 95% ψ_p.	$q_I = \frac{5a^2 B_T}{R\, I_p(MA)} \frac{1+\kappa^2}{2}$ κ is the plasma average elongation at the surface defined by 95% ψ_p.

3.2 Benchmark calculation of INTOR-like design

Japanese delegation has performed a benchmark study reproducing design parameters of INTOR and Next Step Machines of participating countries by using our own systems code. As mentioned in the previous section, there are lots of differences in the plasma physics assumptions. However we tried to reproduce other country's machine design by chainging algorithm and input of the systems analysis code. Table 3.2 shows the design parameters of each INTOR-like designs calculated. Underlined value is the input to the systems analysis code and others are the output. Generally, plasma parameters of each delegation are well reproduced implying that the differences of plasma physics assumptions among the parties are well understood. Fig. 3.1 - 3.4 show calculated results of each INTOR-like device.

For the engineering design, TF and PF coil design parameters are listed in Table 3.2. Electromagnetic quantities are reproduced fairly well. Difference observed is in the evaluation of the stress intensity of the coils. Those difference may come from difference of the conductor design and assumptions made for structural properties, including the load ratio transfered from conductor to coil case.

This benchmark calculation was very useful to understand the differences of physics and engineering approaches of participating countries and to establish the common bases for having single machine design by international cooperation.

Table 3.2.(1) Simulations of INTOR and NET parameters

	INTOR (IAEA) (2)	TRESCODE	NET (EC) (2)	TRESCODE
Plasma				
Plasma major radius (m)	5.0	5.00	5.18	5.18
Plasma minor	1.2	1.20	1.35	1.35
Plasma elongation (avge 95% ψ_p), $\tilde{\kappa}$	1.6 (upper)	1.75	2.05	2.00
Plasma triangularity (avge 95% ψ_p), $\tilde{\delta}$	~0.25	0.2	0.48	0.40
SOL (inboad/outboad) (m)	0.2/0.1	0.2/0.1	0.19/0.13	0.19/0.13
Null-chamber distance (m)	0.9	0.9	1.91	1.91
Plasma volume (m^3)*	227	249	405	406.7
Plasma current (MA)	8.0	8.0	10.8	10.81
Toroidal field on axis (T)	5.5	5.50	5.0	5.0
Safety factor q_I**	1.8	2.01	2.1+	2.23+
Total beta β (%)	4.9	4.85	5.6	5.61
Fuel beta β_{DT} (%)	4.1	4.11	4.2	4.09
Fast α pressure over β (%)	—	5.0	10.0	10.0
Z_{eff}	≤1.5	1.48	2.0	2.05
Plasma temperature (keV)	10.0	10.0	10.0	10.0
Electron density (10^{20} m^{-3})	—	1.83	1.7	1.74
Fuel density (10^{20} m^{-3})	1.3	1.54	1.3	1.26
Fusion power (MW)	585	580	650	632
Neutron wall load (MW/m^2)	~1.2	1.37	1.0	1.08
Alpha heating power (MW)	117	116	130	126
Radiation loss power (MW)	—	24	—	44
Heating power (MW)	50	41	50	48
RF power for start-up (MW)	10	(10)	10	(10)
RF power for current ramp-up (MW)	20++	(20)	—	—

* $Vol = 2\pi^2\tilde{\kappa}a^2R$

** $q_I = \frac{5aB_T}{AI_p(MA)} \frac{1+\tilde{\kappa}^{1/2}}{2}$

\+ Plasma elongation at upper side

++ LHCD power of 20 MW initially installed

+++ $q_I = \frac{5aB_T}{AI_p(MA)} K^2$, $K = \oint \frac{d\ell}{2\pi a}$ at separatrix

Table 3.2.(1) (Continued)

	INTOR (2) (IAEA)	TRESCODE	NET (2) (EC)	TRESCODE
TF COIL				
Superconductor material	Nb_3Sn	Nb_3Sn	Nb_3Sn	Nb_3Sn
Number of coils	12	12	16	16
Ripple at plasma edge (%)	1.2	1.4	1.2	~1.1
Bore (horizontal) (m)	6.3	6.29	6.0	5.94
(vertical) (m)	—	8.63	11.0	10.7
Perimeter per coil (m)	—	26.8	—	30.5
Inner leg position (m)	2.41	2.41	2.13	2.20
TFC thickness at inner leg (m)	0.67	0.67	0.7	0.692
Max. field (T)	11.0	11.6	11.4	11.4
Max. current density in conductor (A/mm^2)	25.0	33.8	22	24.0
Average current density (A/mm^2)	—	$11.1^{+}/14.1^{++}$	13.8	14.0
Total current (MA)	—	137.6	130	129
Ampere-turn meter (GATM)	—	3.69	—	3.9
Stored energy (GJ)	—	21.3	25	23.1
Inplane centering force (MN/m)	—	60.9	—	42.1
Inplane vertical force (GN/m)	—	2.54	—	2.3
Max. overturning force (MN/m)	—	34.4	—	24.2
Average tensile stress of TFC case (MPa)*	—	218	—	324
Average tensile stress of conductor (MPa)**	—		(150)	140
Average compressive stress of B.C. (MPa)	—	42^{+++}	×	×
Allowable buckling stress of B.C (MPa)	—	282^{+++}	×	×
Total nuclear heating (kW)	15	5.71	8.0	~2.0
Total AC loss, etc (kW)	—	(40.0)	—	(40.0)
Nuclear heating rate (mW/cc)	—	0.6	—	0.1
Radiation dose on insulator (rad)	$10^8/10^{10}$	$1.5 \cdot 10^8$	—	$3.1 \cdot 10^8$

* $\sigma_1 = F_z/2 \cdot A_{TFC}$, F_z : vertical force

A_{TFC}: total cross-sectional area at inner leg.

** $\sigma_1 = 0.7\ F_z/2 \cdot A_{con}$

A_{con}: winding pack area of TFC.

\+ Including Bucking cylinder as well as He can.

++ Excluding Bucking cylinder

+++ Bucking cylinder thickness assumed 0.23 m.

Table 3.2.(1) (Continued)

	INTOR (IAEA) (2)	TRESCODE	NET (EC) (2)	TRESCODE
PF COIL				
Superconductor materials	Nb_3Sn	Nb_3Sn	Nb_3Sn	Nb_3Sn
Maximum current density (A/mm^2)	—	30.0		30.0
Peak field in solenoid (T)	8	8	11/9	11.0
Selenoid end-radius (m)	1.70	1.70		1.75
Selenoid thickness (m)	0.55	0.55	0.6	0.425(0.60)
Total available volt seconds (v.s)	(112)	150 (10T)+	181	185
Burn time-non-inductive (s)	—	—	—	—
-full-inductive (s)	200	290	350	~200
PF coil current sum at minimum (MA)	—	62.6	—	101
Sum of max. PF coil currents (MA)	—	146.3	—	~200
Maximum Ampere-turn meter (GATM)	—	3.25	—	3.75
Stored energy at $\psi_p = 0$ (GJ)	14	6.0	5.5	5.7
Power supply				
Total convertor capacity for PFC (GW)	—	4.1++	—	4.9+
Total transformer capacity for PFC (GMVA)	—	6.3++	—	7.4+
A.C Power supply for heating (MVA)	—	126	—	230
Figure of merits				
Relative cost to INTOR (%)	100	100	—	109
Ignition margins - ASDEX-H	—	1.72	—	1.29
I_g* MIRNOV-type	—	1.01	—	0.93
Kaye-Goldstron	—	0.63	—	0.54
JAERI	—	1.31	—	0.92
INTOR	—	1.14	—	0.95

* Definition of I_g ;

SUPERCOIL : $I_g \equiv P_\alpha/P_{con}$, $P_{con} = 3kn_DT/\tau_E$

TRESCODE : $I_g \equiv (P_\alpha - P_{rad})/P_{con}$, $P_{con} = \frac{3}{2}(n_e+n_i)T/\tau_E$

\+ Allowable feak field is assumed 10 T.

++ Plasma break down: 35 V · 0.3 sec

Table 3.2.(2) Simulations of TIBER and OTR parameters

	TIBER (2) (US)	TRESCODE	OTR (2) (USSR)	TRESCODE
Plasma				
Plasma major radius (m)	3.03	3.00	6.3	6.31
Plasma minar radius (m)	0.83	0.83	1.5	1.51
Plasma elongation (avge 95% ψ_p), $\tilde{\kappa}$	2.4	2.4	1.5	1.5
Plasma triangularity (avge 95% ψ_p), $\tilde{\delta}$	0.4	0.4	0.3	0.3
SOL (inboad/outboad) (m)	0.09/0.09	0.09/0.09	0.3/0.1	0.3/0.1
Null-chamber distance (m)	0.15	0.15	0.7	0.7
Plasma volume* (m^3)	–	99		428
Plasma current (MA)	10	10.0	8.0	8.0
Toroidal field on axis (T)	5.55	5.6	5.8	5.7
Safety factor q_I		2.19	2.1	2.1
Total beta β (%)	6	6.0	3.2	3.25
Fuel beta β_{DT} (%)	4.3	4.3	2.7	2.81
Fast α pressure over β (%)	–	18.8	–	2.0
Z_{eff}	2.09	2.02	1.5	1.48
Plasma temperature (keV)	19.6/19.2 ++	19.2 +++	8	8.0
Electron density (10^{20} m^{-3})	–	1.12	–	1.69
Fuel density (10^{20} m^{-3})	0.796	0.88	1.4	1.41
Fusion power (MW)	279	273	500	533
Neutron wall load (MW/m^2)	–	1.20	–	0.89
Alpha heating power (MW)	55.8	55.0	100	106
Radiation dose power (MW)	–	15.9	–	30
Heating power (MW)	20(+50) ++++	30	50	67.5
RF power for start-up (MW)	10	10	10	10
RF power for carrent ramp-up (MW)	20	20	–	–

* $Vol = 2\pi^2 \kappa a^2 R$

** $q_I = \frac{5aB_T}{A I_p(MA)} \cdot \frac{1+\tilde{\kappa}^2}{2}$

\+ Volume within separatrix

++ T_i = 19.6 keV, T_e = 19.2 keV

+++ $T_e = T_i$ is assumed

++++ NBI power of 50 MW will be added as a option.

Table 3.2.(2) (Continued)

	TIBER (2) (US)	TRESCODE	OTR (2) (USSR)	TRESCODE
TF COIL				
Superconductor naterial	Nb_3Sn	Nb_3Sn	Nb_3Sn	Nb_3Sn
Number of coils	16	16	12	12
Ripple at plasma edge (%)	0.8	0.8	1	~1.0
Bore (horizontal) (m)	3.7	3.7	7.7	7.9
(vertical) (m)	6.6	6.45	10.8	10.8
Perimeter per coil (m)	-	18.3	-	33.3
Inner leg position (m)	1.312	1.32	2.7	2.74
TFC thickness (m)	0.49	0.485	1.1	1.1
Max. current density in conductor (A/mm^2)	40	41.0	35	35.0
Average current density (A/mm^2)	22.2	21.1	-	
Total current (MA)	90	84.2	180	179
Ampere-turn meter (GATM)	-	1.54	-	5.96
Stored energy (GJ)	4	6.0	45	48.5
Inplane centering force (MN/m)		29.5	-	89.7
Inplane vertical force (GN/m)		1.0	-	4.7
Max. overturning force (MN/m)		9.3	-	44.9
Average tensile stress of TFC case (MPa)*		257	-	160
Average tensile stress of conductor (MPa)**			-	
Average compressive stress of B.C		(23.5)+	×	×
Allowable buckling stress of B.C		(786)	×	×
Total nuclear heating (kW)	72++	119	15	0.07
Total AC loss (kW)	-	(40.0)	-	(40.0)
Nuclear heating rate (mW/cc)	5++	9.95	1	0.02
Radiation dose on insulator (rad)	-	$3.6 \cdot 10^8$	-	$1.0 \cdot 10^7$

* $\sigma_1 = F_z/2 \cdot A_{TFC}$, F_z : vertical force

A_{TFC}: total cross sectional area at inner leg

** $\sigma_1 = 0.7 \cdot F_z/2 \cdot A_{con}$

A_{con}: winding pack area of TFC

\+ Bucking cylinder thickness is assumed 0.23 m.

++ Tangsten shield

Table 3.2.(2) (Continued)

	TIBER (US)[2]	TRESCODE	OTR (USSR)[2]	TRESCODE
PF COIL				
Saperconductor materials	$(NbTi)_3Sn$	$(NbTi)_3Sn$	NbTi	NbTi
Maximum current density (A/mm^2)		37.0	-	27.0
Peak field in solenoid (T)	14	14.0	8/6	8.0
Selenoid end-radius (m)	1.0	1.0	2.2	2.17
Selenoid thickness (m)	0.4	0.4	0.4	0.37
Total available volt seconds (v.s)	58	68.7	210	212
Burn time-non-inductive (s)	-	1700	-	-
-full-inductive (s)	-	-	600	~500
PF coil current sum at minimum (MA)	-	85.7	-	101
Sum of max. PF coil currents (MA)	-	130.9	-	148
Maximum Ampere-turn meter (GATM)	-	1.72	-	4.68
Stored energy at $\psi_p=0$ (GJ)	4	4	9	11
Power supply				
Total convertor capacity for PFC (GW)	-	1.2+	-	2.9
Total transformer capacity for PFC (GVA)	-	1.8+	-	4.5
A.C Power supply for heating (MVA)	-	143	-	324
Figure of merits				
Relative cost to INTOR (%)	-	71	-	138
Ignition margins-ASDEX-H	-	1.13	-	0.90
I_q* MIRNOV-type	-	0.82	-	0.46
Kaye-Goldston	-	0.51	-	0.30
JAERI	-	0.47	-	0.73
INTOR	-	0.44	-	0.56

* Definition of I_g ;

SUPERCOIL : $I_g \equiv P_\alpha/P_{con}$, $P_{con} = 3kn_DT/\tau_E$

TRESCODE : $I_g \equiv (P_\alpha - P_{rad})/P_{con}$, $P_{con} = \frac{3}{2}(n_e + n_i)T/\tau_E$

\+ Plasma break down: 10 V·1 sec

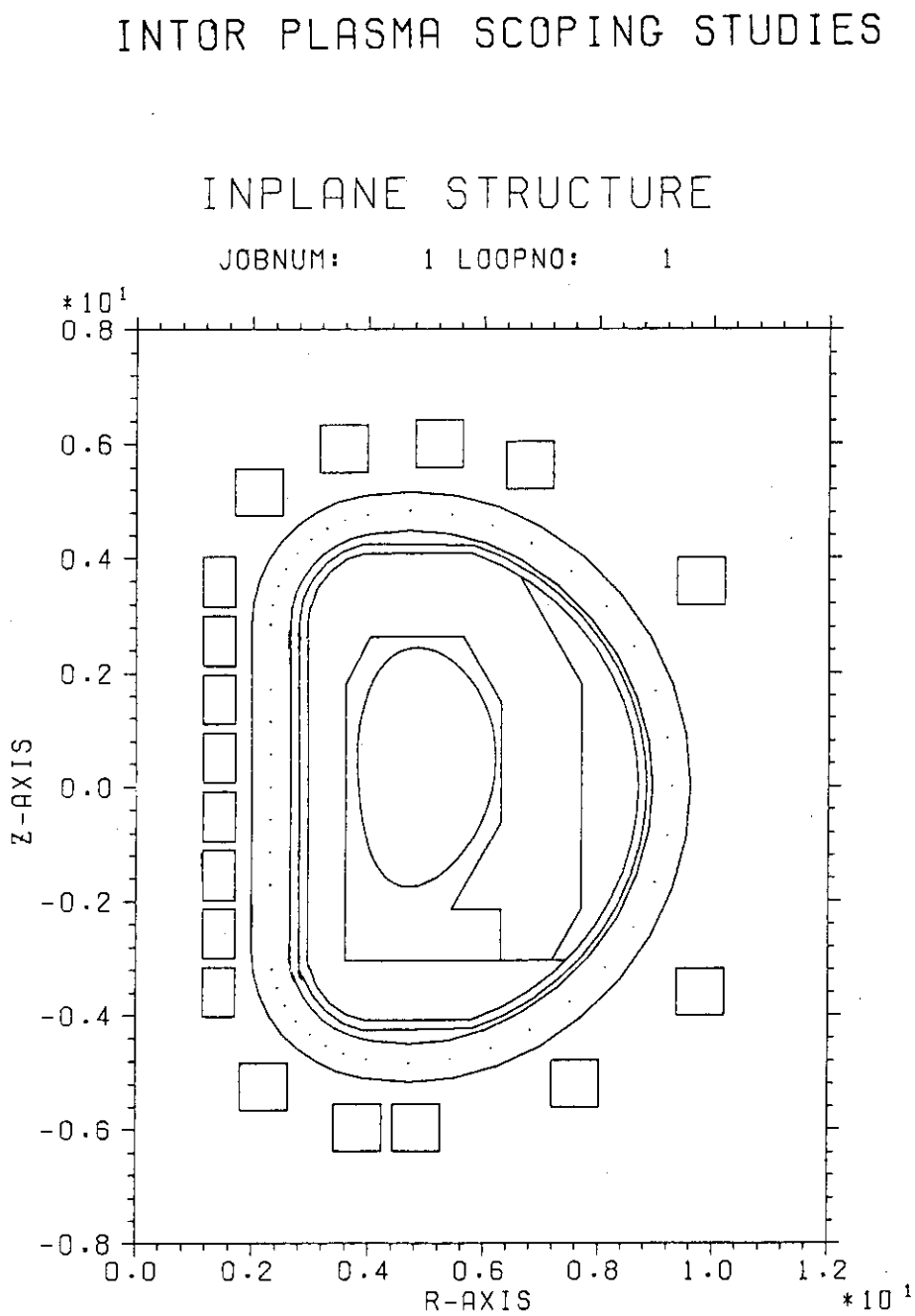

Fig. 3.1 (1) INTOR inplane core structure

INTOR PLASMA SCOPING STUDIES

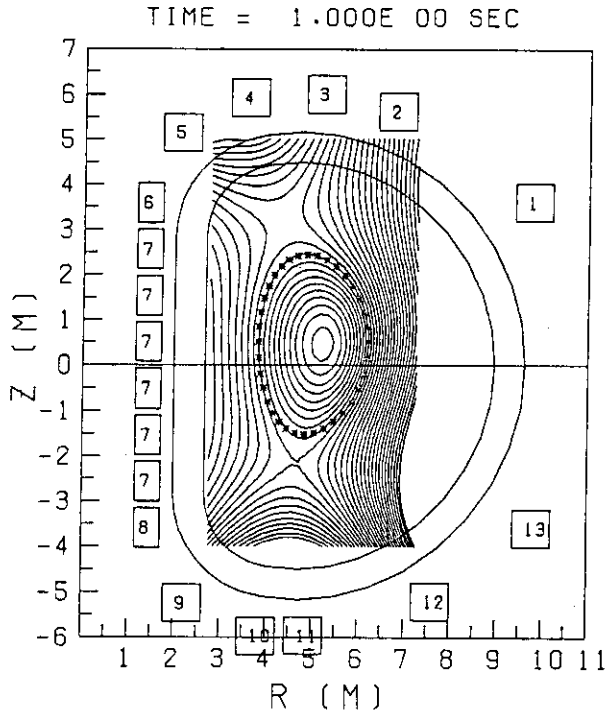

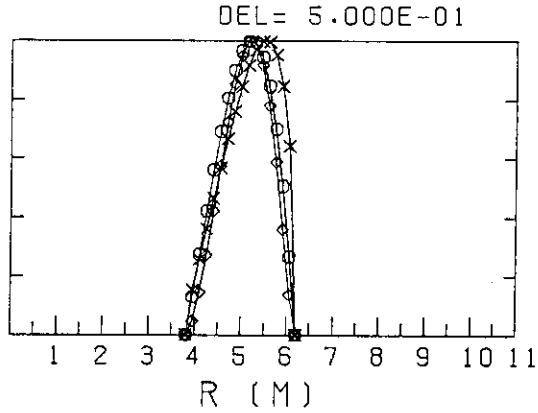

MAG.FLUX MAX= 1.578E 01.SURFACE= 1.104E 01

CUR.DENST. MAX= 1.962E 06 A/M**2

PRESSUR MAX= 1.696E 06 N/M**2

***** PLASMA PARAMETERS *********

IP-CURRENT	(A)	8.003E 06
VLOOP-SURFACE	(V)	-6.937E 01
SELF INDUCTANCE	(H)	1.078E-05
SMALL LI		8.766E-01
R-AVERAGE	(M)	5.008E 00
R-INNER	(M)	3.816E 00
R-OUTER	(M)	6.200E 00
R-MAGNETIC AXIS	(M)	5.203E 00
R-CURRENT MAX.	(M)	5.514E 00
A-HALF WIDTH	(M)	1.192E 00
A-AVERAGE	(M)	1.577E 00
ELLIPTICITY		1.749E 00
CROSS AREA	(M**2)	7.809E 00
VOLUME	(M**3)	2.425E 02
TOROLDAL BETA	(MHD)	4.848E-02
POLOIDAL BETA	(MHD)	2.651E 00
POLOIDAL BETA	(AREA)	1.792E 00
POLOIDAL BETA	(VOLUME)	1.840E 00
Q-VALUE	(MHD)	3.705E 00
BV-SHAFRANOV	(T)	-6.158E-01
BV-CALCULATED	(T)	-5.548E-01
SUPPLIED FLUX	(WB)	1.106E-04
ABS TOTAL AMP	(AT)	8.923E 07
STORED ENERGY	(J)	6.160E 09
AMP-T METER	(AT-M)	2.302E 09
LIMITER R	(M)	4.635E 00
Z	(M)	-2.141E 00
PSI	(WB)	1.104E 01
RP (95%)	(M)	5.020E 00
AP (95%)	(M)	1.152E 00
ZP (95%)	(M)	4.637E-01
ELON-UPPER	(95%)	1.655E 00
ELON-LOWER	(95%)	1.955E 00
TRIANG-UPPER	(95%)	1.456E-01
TRIANG-LOWER	(95%)	2.759E-01

Fig. 3.1 (2) INTOR plasma equilibrium calculation

INTOR PLASMA SCOPING STUDIES

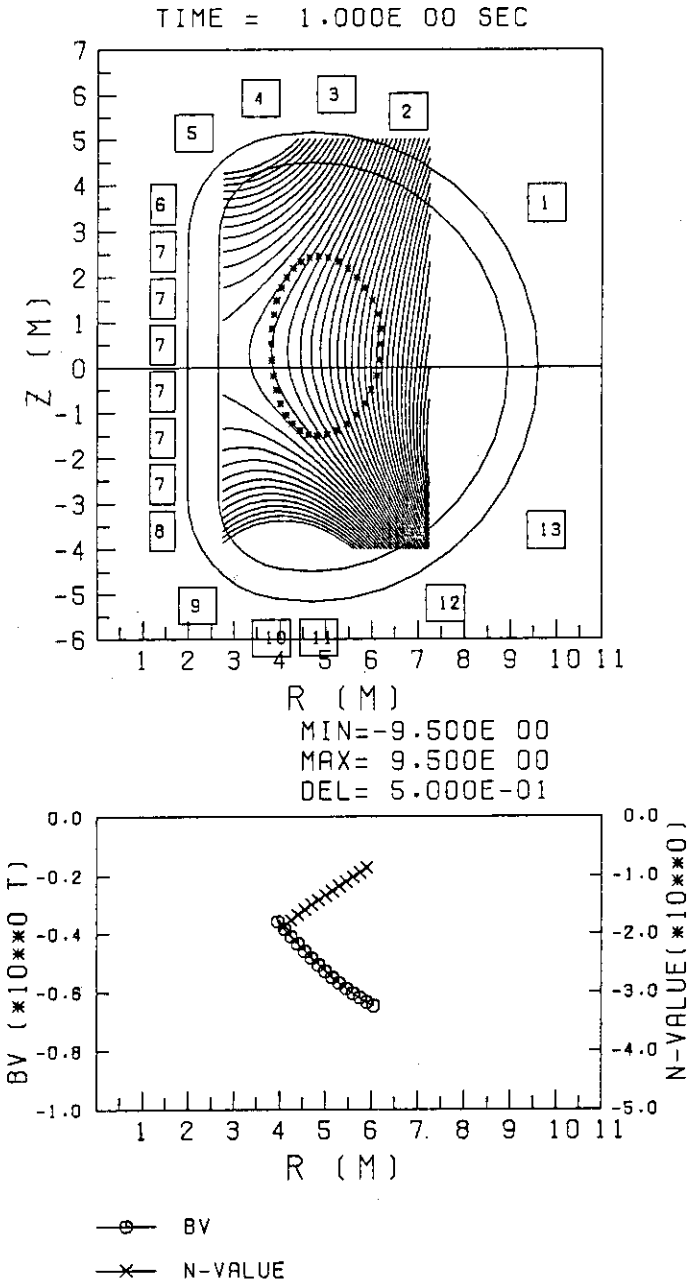

***** COILS **********

NO.	CURRENT(A)	BV(T)
1	-4.083E 06	-2.465E-01
2	-1.009E 05	-3.306E-03
3	1.092E 06	2.057E-02
4	6.176E 06	5.059E-02
5	1.183E 07	2.635E-02
6	6.302E 06	-2.279E-03
7	2.584E 06	-4.996E-02
8	1.624E 06	1.027E-03
9	8.647E 06	2.342E-02
10	9.531E 06	7.802E-02
11	9.988E 06	1.324E-01
12	2.069E 06	6.707E-02
13	-1.228E 07	-6.237E-01

Fig. 3.1 (3) INTOR external field calculation

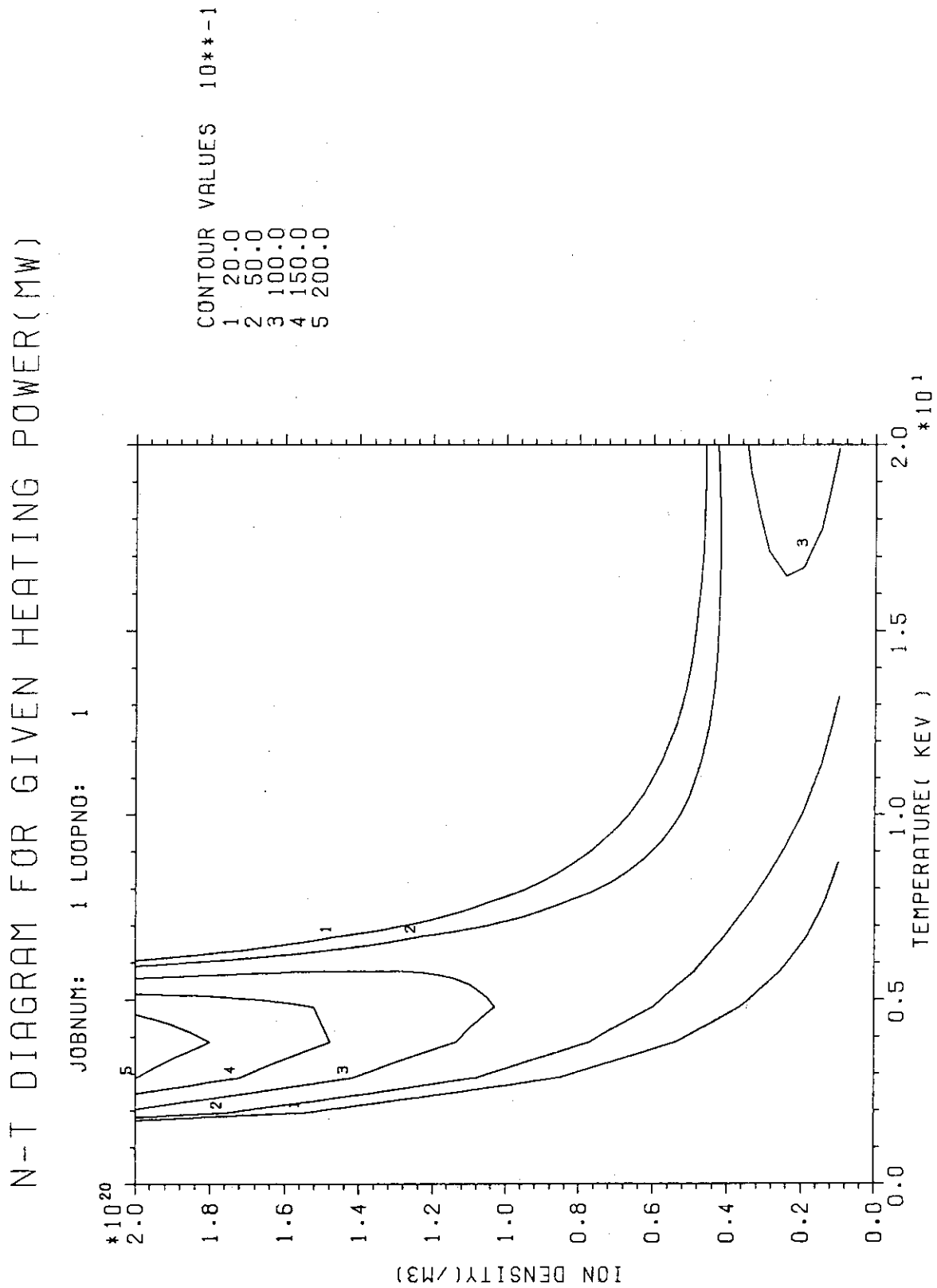

Fig. 3.1 (4) INTOR plasma n-T diagram

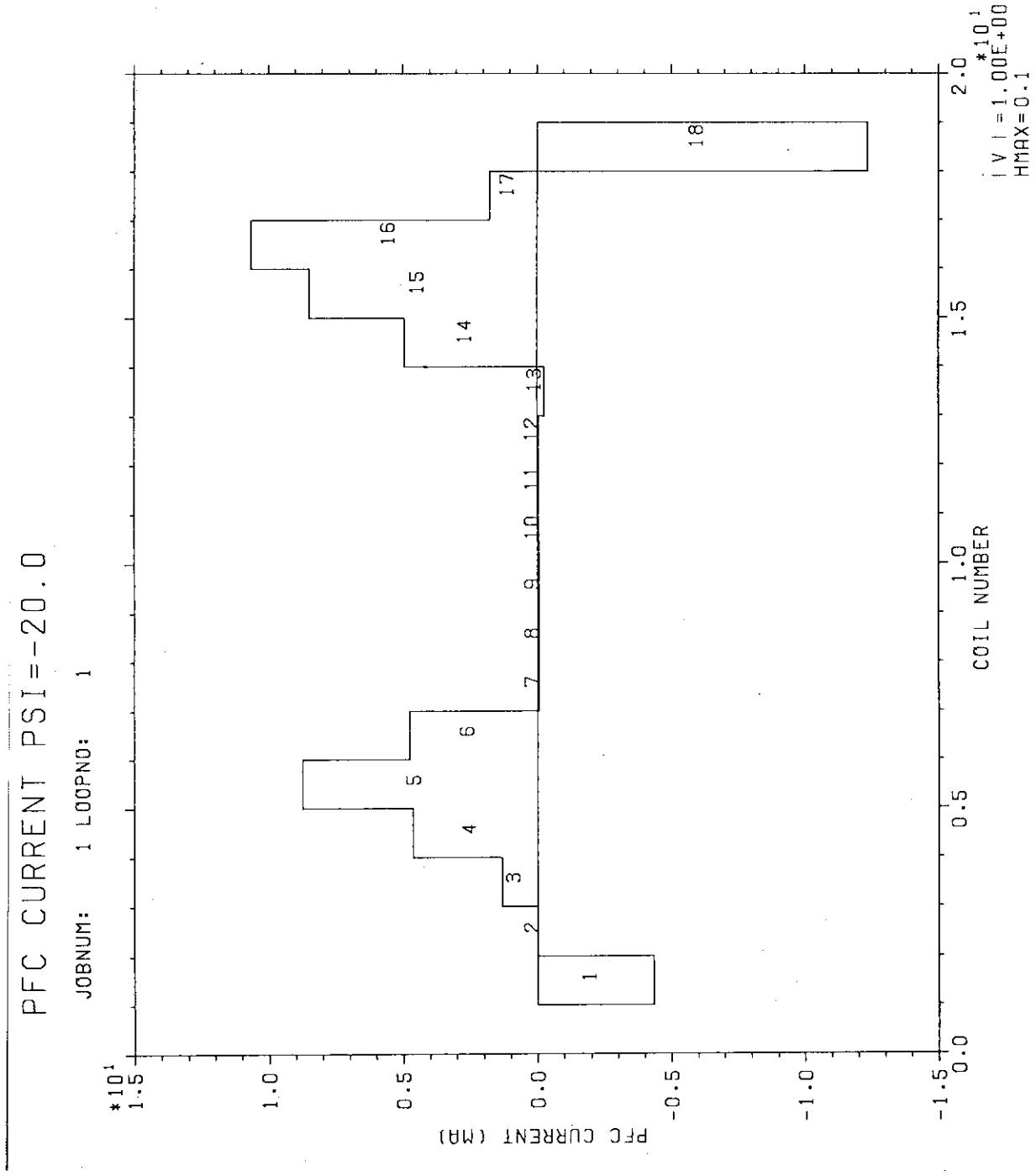

Fig. 3.1 (5) INTOR PF coil current pattern at Ψ_p = -20 v.s

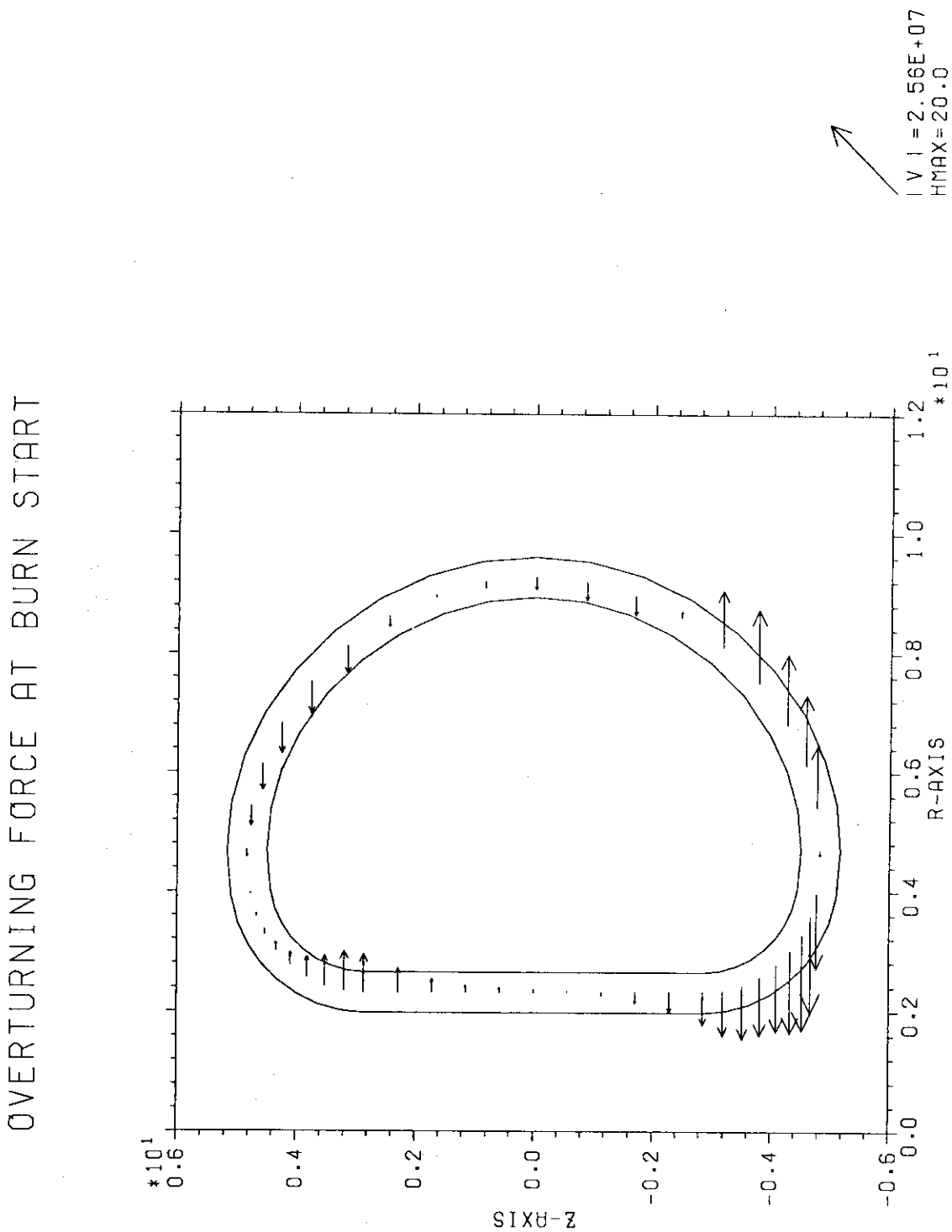

Fig. 3.1 (6) INTOR overturning force on TFC

INTOR SCOPING STUDIES

BENCHMARK STUDIES FOR NET

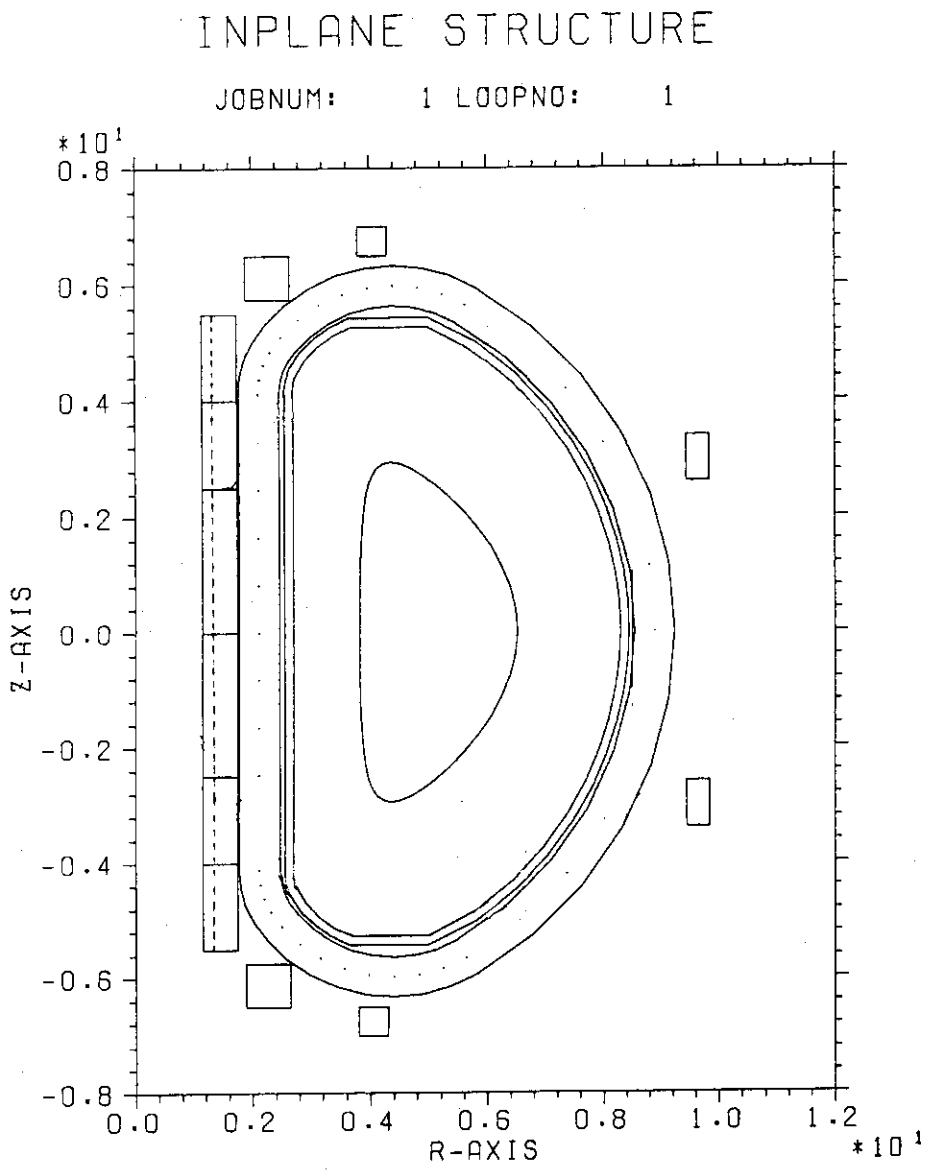

Fig. 3.2 (1) NET inplane core structure

BENCHMARK STUDIES FOR NET PARAMETERS

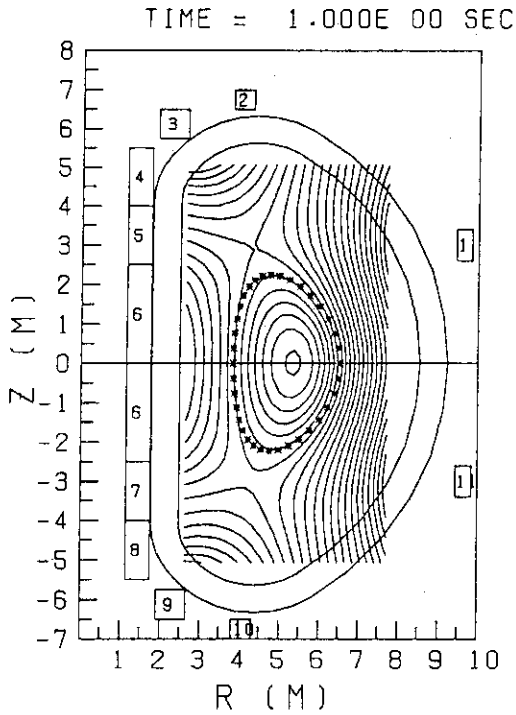

***** PLASMA PARAMETERS *********

IP-CURRENT	(A)	1.082E 07
VLOOP-SURFACE	(V)	-8.653E 01
SELF INDUCTANCE	(H)	9.985E-06
SMALL LI		8.753E-01
R-AVERAGE	(M)	5.160E 00
R-INNER	(M)	3.853E 00
R-OUTER	(M)	6.467E 00
R-MAGNETIC AXIS	(M)	5.328E 00
R-CURRENT MAX.	(M)	5.621E 00
A-HALF WIDTH	(M)	1.307E 00
A-AVERAGE	(M)	1.845E 00
ELLIPTICITY		1.993E 00
CROSS AREA	(M**2)	1.070E 01
VOLUME	(M**3)	3.379E 02
TOROLDAL BETA	(MHD)	5.610E-02
POLOIDAL BETA	(MHD)	2.403E 00
POLOIDAL BETA	(AREA)	1.374E 00
POLOIDAL BETA	(VOLUME)	1.417E 00
Q-VALUE	(MHD)	4.730E 00
BV-SHAFRANOV	(T)	-7.006E-01
BV-CALCULATED	(T)	-6.246E-01
SUPPLIED FLUX	(WB)	1.770E-04
ABS TOTAL AMP	(AT)	1.407E 08
STORED ENERGY	(J)	8.966E 09
AMP-T METER	(AT-M)	2.338E 09
LIMITER R	(M)	4.299E 00
Z	(M)	2.939E 00
PSI	(WB)	1.377E 01
RP (95%)	(M)	5.170E 00
AP (95%)	(M)	1.265E 00
ZP (95%)	(M)	2.811E-04
ELON-UPPER	(95%)	2.020E 00
ELON-LOWER	(95%)	1.980E 00
TRIANG-UPPER	(95%)	3.965E-01
TRIANG-LOWER	(95%)	3.965E-01

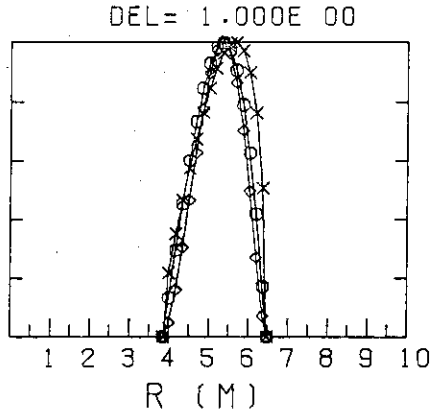

MAG.FLUX MAX= 1.995E 01.SURFACE= 1.377E 01

CUR.DENST. MAX= 1.885E 06 A/M**2

PRESSUR MAX= 1.673E 06 N/M**2

Fig. 3.2 (2) NET plasma equilibrium calculation

BENCHMARK STUDIES FOR NET PARAMETERS

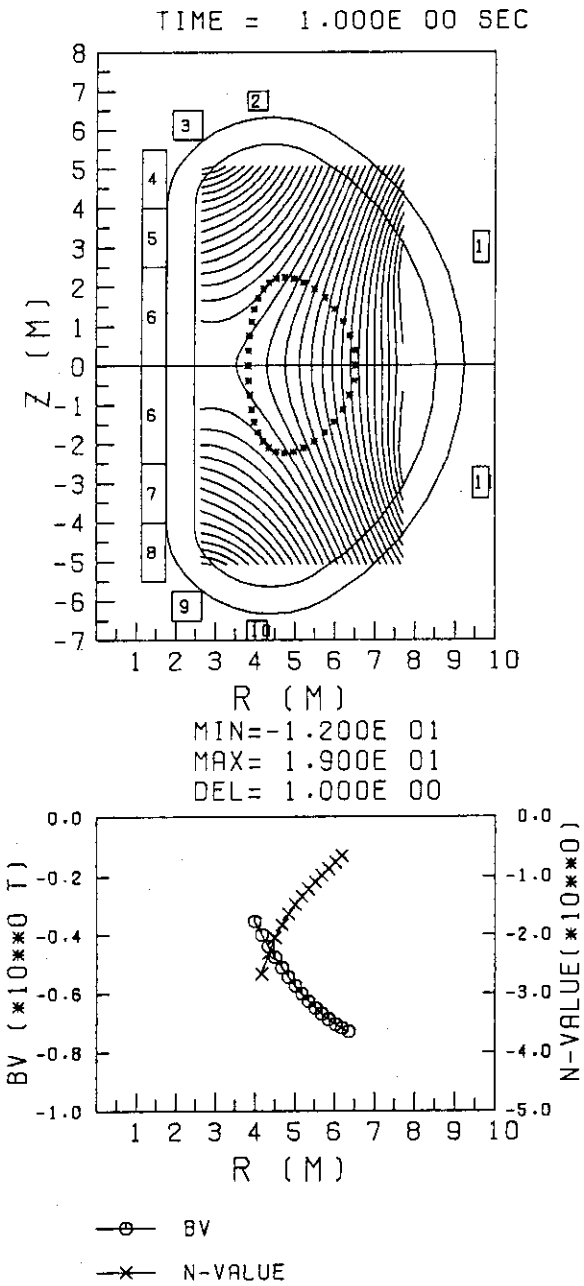

***** COILS **********

NO.	CURRENT(A)	BV(T)
1	-6.476E 06	-3.883E-01
2	2.839E 06	2.429E-02
3	2.847E 07	7.838E-02
4	1.584E 07	1.472E-02
5	1.555E 07	-2.046E-03
6	2.099E 06	-1.692E-02
7	1.712E 07	-2.251E-03
8	1.487E 07	1.381E-02
9	2.466E 07	6.790E-02
10	4.312E 06	3.689E-02
11	-6.403E 06	-3.839E-01

Fig. 3.2 (3) NET external field calculation

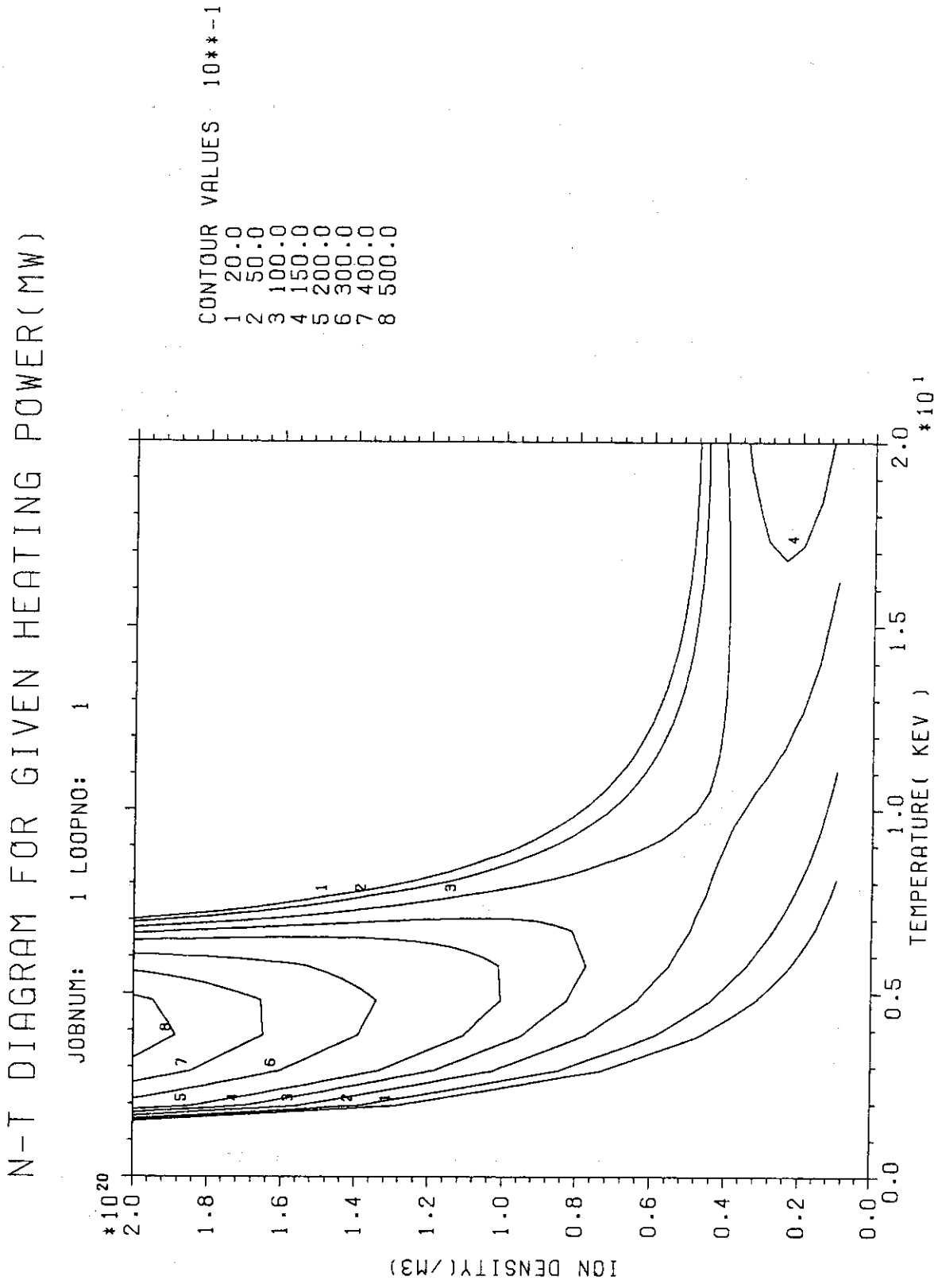

Fig. 3.2 (4) NET plasma n-T diagram

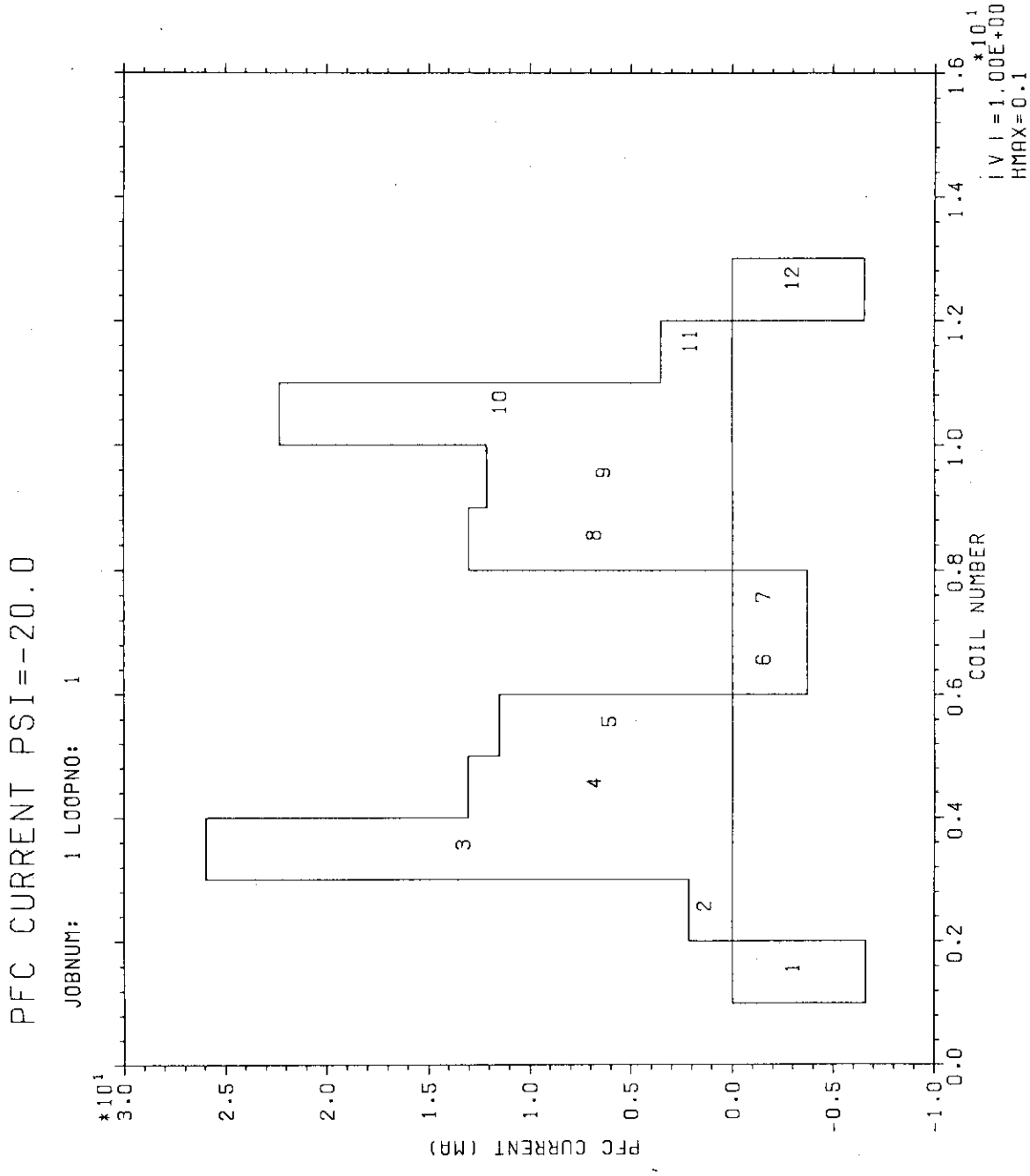

Fig. 3.2 (5) NET PF coil current pattern at Ψ_p = -20 v.s

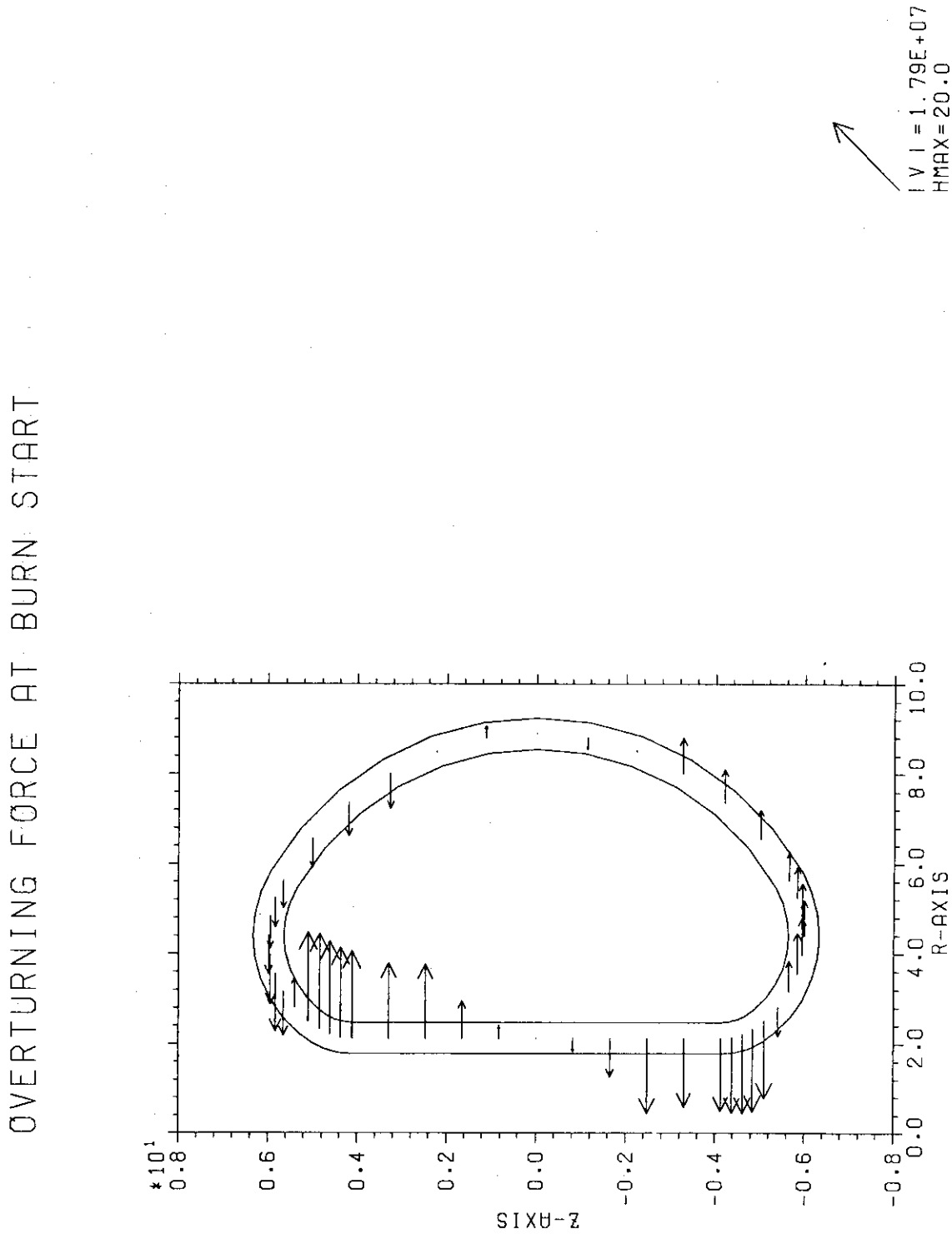

Fig. 3.2 (6) NET overturning force on TFC

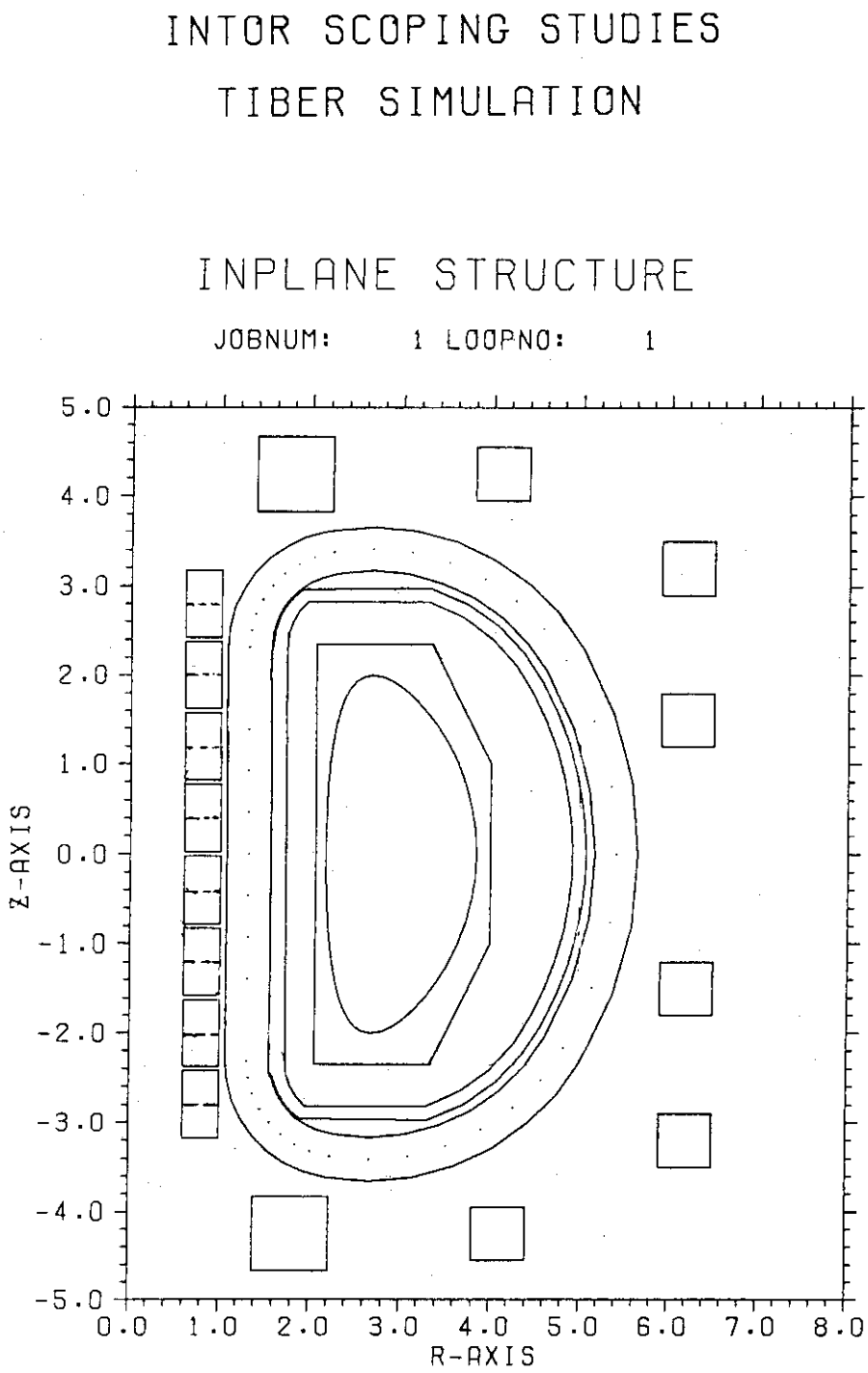

Fig. 3.3 (1) TIBER inplane core structure

INTOR SCOPING STUDIES

TIBER SIMULATION

TIME = 1.000E 00 SEC

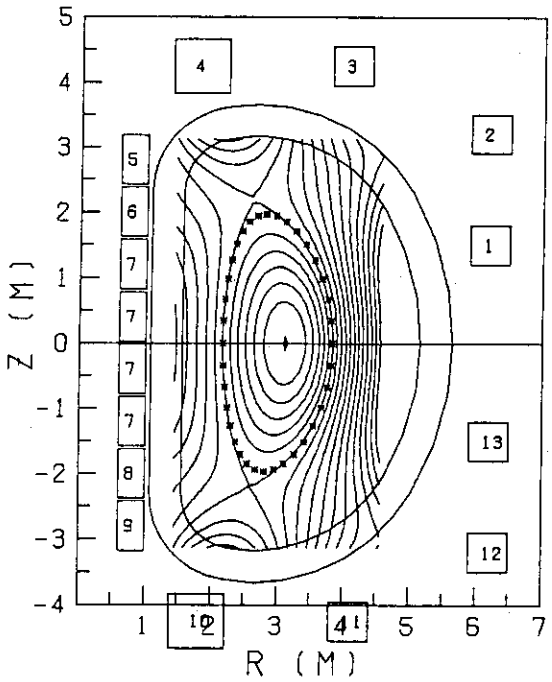

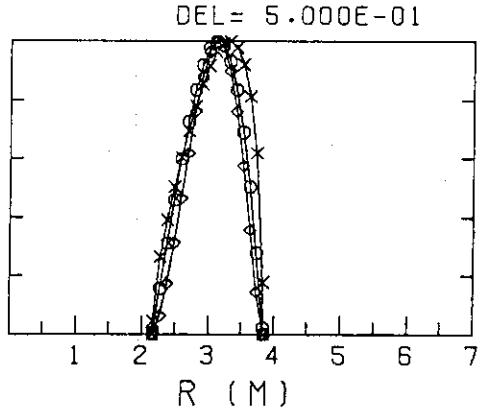

MAG.FLUX MAX= 9.484E 00.SURFACE= 6.469E 00

CUR.DENST. MAX= 3.475E 06 A/M**2

PRESSUR MAX= 2.263E 06 N/M**2

***** PLASMA PARAMETERS *********

IP-CURRENT	(A)	1.003E 07
VLOOP-SURFACE	(V)	-4.065E 01
SELF INDUCTANCE	(H)	5.096E-06
SMALL LI		8.467E-01
R-AVERAGE	(M)	3.003E 00
R-INNER	(M)	2.163E 00
R-OUTER	(M)	3.842E 00
R-MAGNETIC AXIS	(M)	3.118E 00
R-CURRENT MAX.	(M)	3.286E 00
A-HALF WIDTH	(M)	8.394E-01
A-AVERAGE	(M)	1.296E 00
ELLIPTICITY		2.382E 00
CROSS AREA	(M**2)	5.274E 00
VOLUME	(M**3)	9.738E 01
TOROLDAL BETA	(MHD)	5.999E-02
POLOIDAL BETA	(MHD)	2.104E 00
POLOIDAL BETA	(AREA)	1.146E 00
POLOIDAL BETA	(VOLUME)	1.183E 00
Q-VALUE	(MHD)	5.323E 00
BV-SHAFRANOV	(T)	-9.738E-01
BV-CALCULATED	(T)	-8.820E-01
SUPPLIED FLUX	(WB)	1.914E-04
ABS TOTAL AMP	(AT)	1.373E 08
STORED ENERGY	(J)	3.992E 09
AMP-T METER	(AT-M)	2.113E 09
LIMITER R	(M)	2.601E 00
Z	(M)	-2.199E 00
PSI	(WB)	6.469E 00
RP (95%)	(M)	3.010E 00
AP (95%)	(M)	8.122E-01
ZP (95%)	(M)	-1.142E-04
ELON-UPPER	(95%)	2.362E 00
ELON-LOWER	(95%)	2.368E 00
TRIANG-UPPER	(95%)	2.682E-01
TRIANG-LOWER	(95%)	2.682E-01

Fig. 3.3 (2) TIBER plasma equilibrium calculation

INTOR SCOPING STUDIES

TIBER SIMULATION

TIME = 1.000E 00 SEC

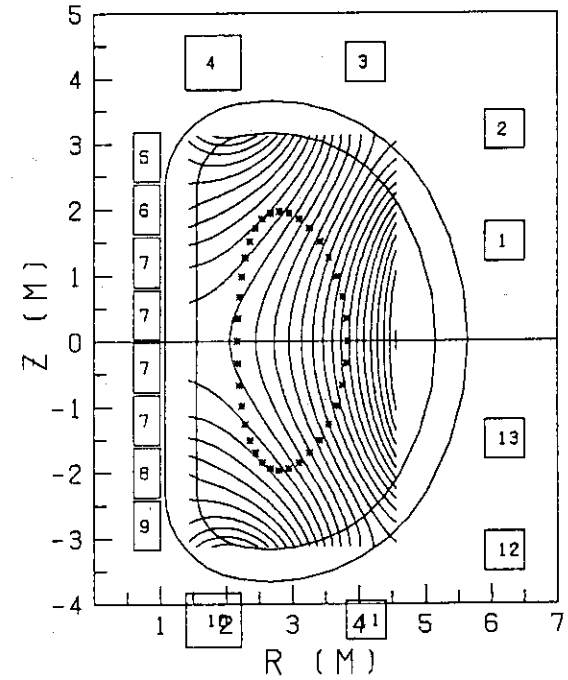

MIN=-6.500E 00
MAX= 6.500E 00
DEL= 5.000E-01

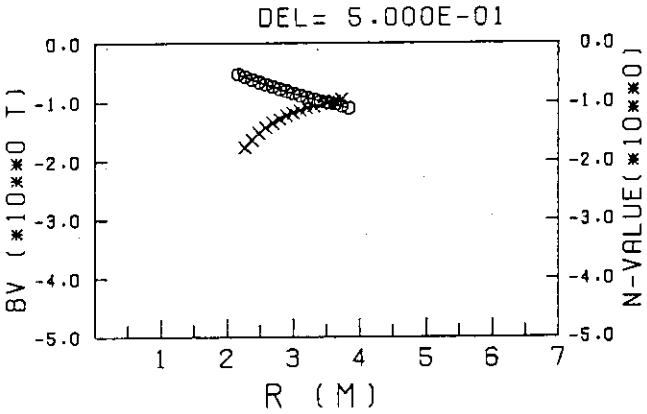

—⊖— BV

—×— N-VALUE

***** COILS **********

NO.	CURRENT(A)	BV(T)
1	-7.884E 06	-8.263E-01
2	6.004E 06	4.110E-01
3	-4.540E 06	-1.588E-01
4	2.344E 07	1.770E-01
5	8.849E 06	1.144E-02
6	1.138E 07	-9.628E-04
7	3.285E 06	-7.078E-02
8	1.131E 07	-9.562E-04
9	8.857E 06	1.145E-02
10	2.358E 07	1.780E-01
11	-4.562E 06	-1.596E-01
12	5.938E 06	4.065E-01
13	-7.839E 06	-8.215E-01

Fig. 3.3 (3) TIBER external field calculation

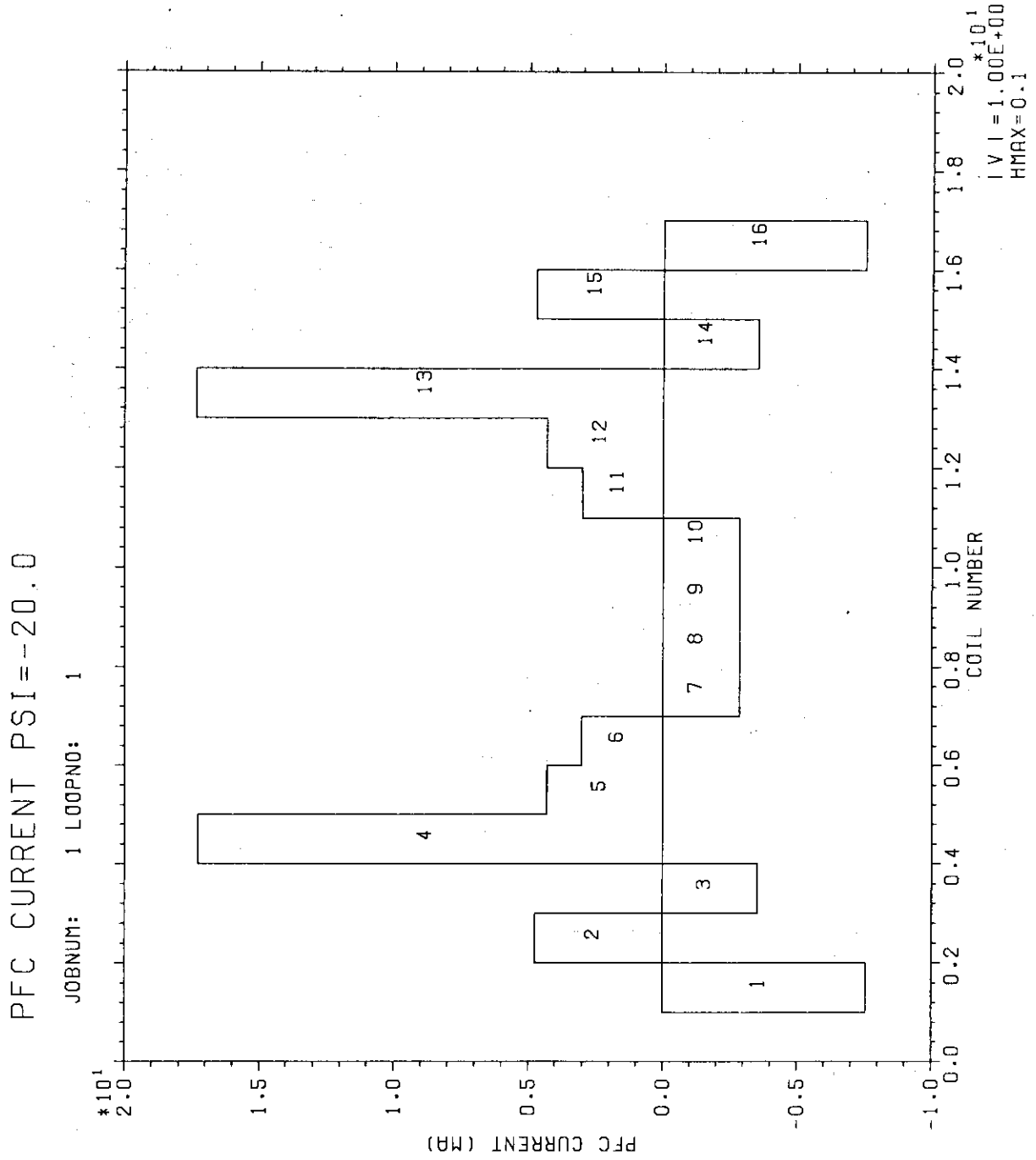

Fig. 3.3 (4) TIBER PF coil current pattern at Ψ_p = -20 v.s

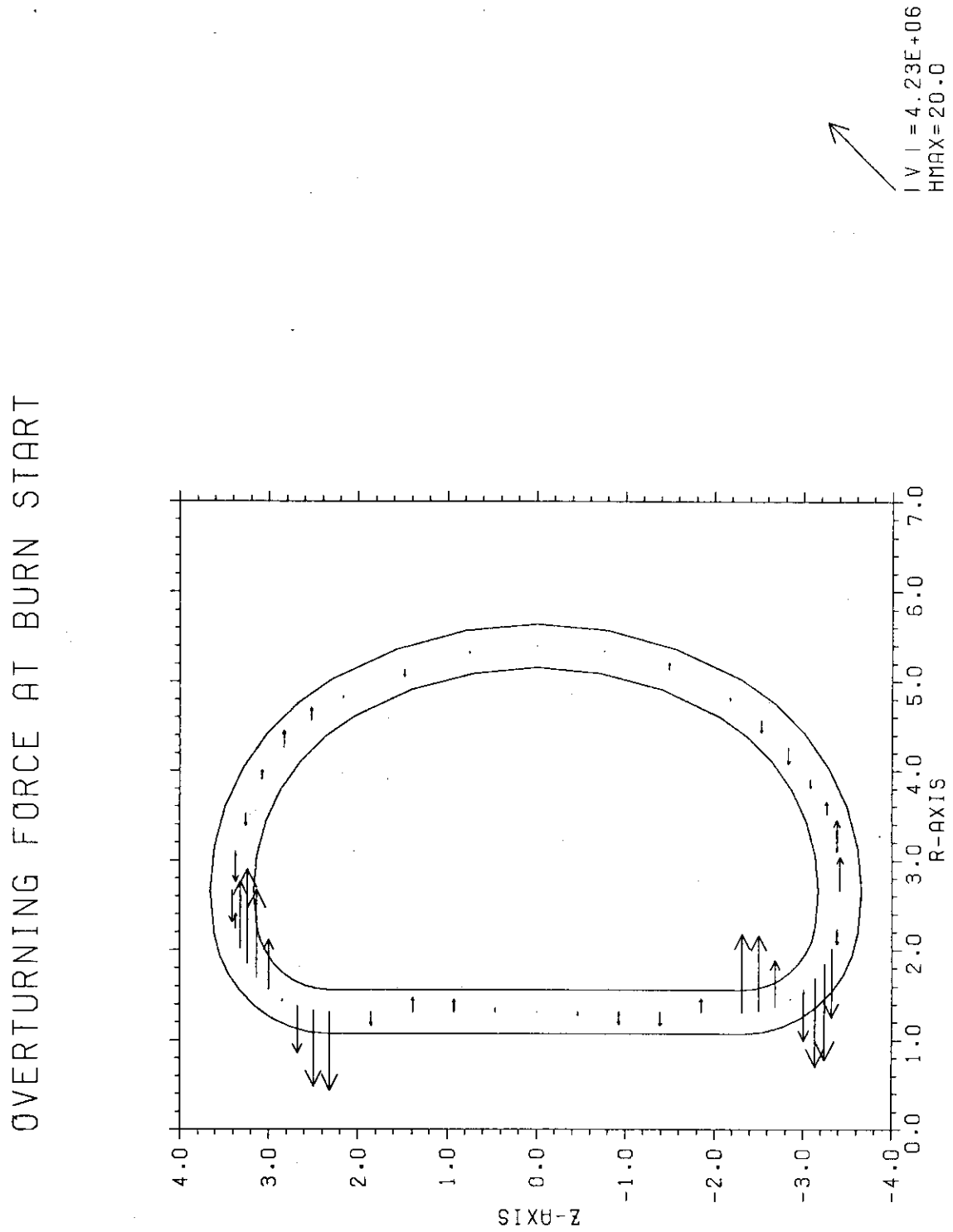

Fig. 3.3 (5) TIBER overturning force on TFC

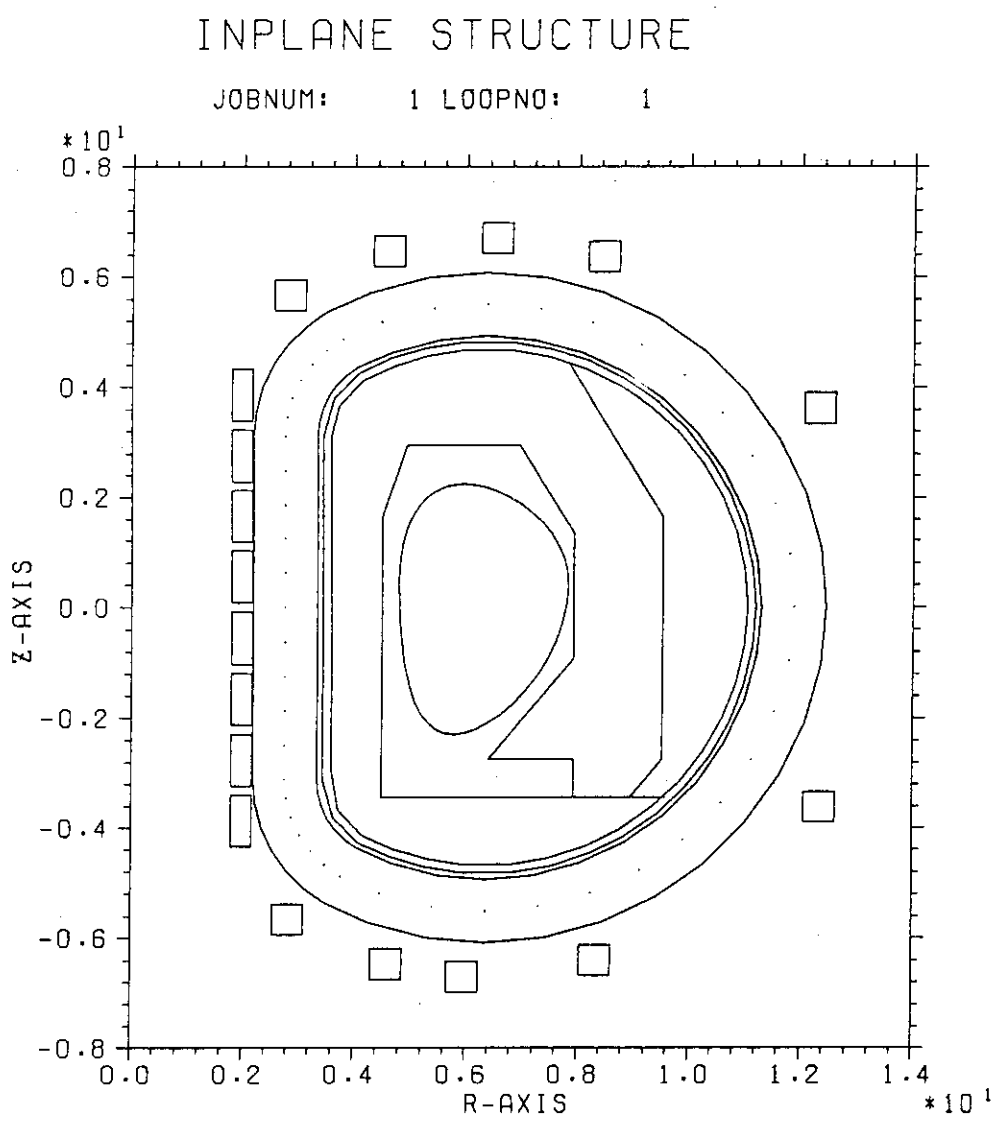

Fig. 3.4 (1) OTR inplane core structure

INTOR SCOPING STUDIES

OTR SIMULATION

TIME = 1.000E 00 SEC

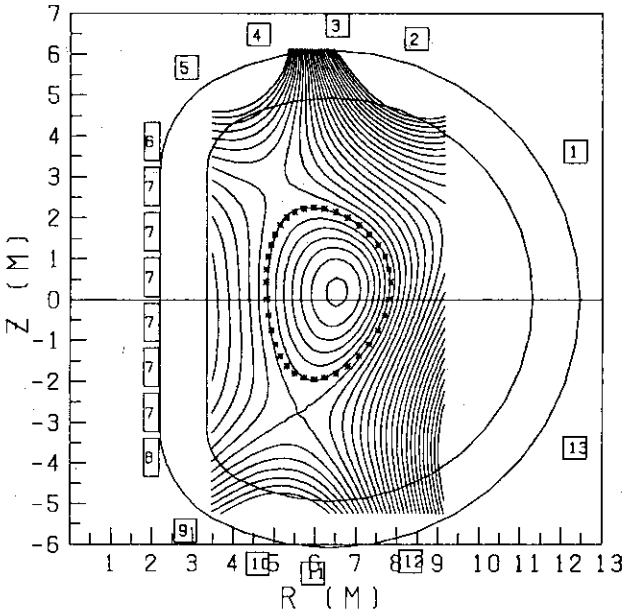

MIN=-5.572E 00
MAX= 2.043E 01
DEL= 1.000E 00

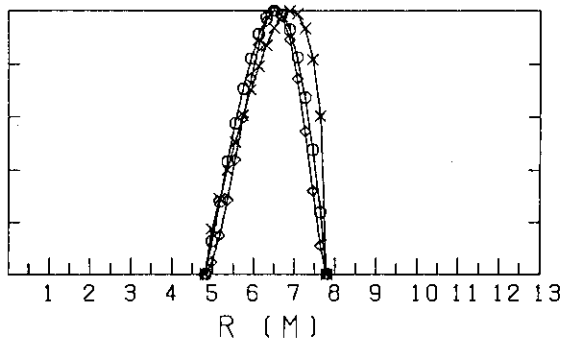

MAG.FLUX MAX= 2.057E 01.SURFACE= 1.443E 01

CUR.DENST. MAX= 1.416E 06 A/M**2

PRESSUR MAX= 1.222E 06 N/M**2

***** PLASMA PARAMETERS *********

IP-CURRENT	(A)	8.011E 06
VLOOP-SURFACE	(V)	-9.066E 01
SELF INDUCTANCE	(H)	1.408E-05
SMALL LI		8.834E-01
R-AVERAGE	(M)	6.304E 00
R-INNER	(M)	4.817E 00
R-OUTER	(M)	7.792E 00
R-MAGNETIC AXIS	(M)	6.517E 00
R-CURRENT MAX.	(M)	6.888E 00
A-HALF WIDTH	(M)	1.487E 00
A-AVERAGE	(M)	1.838E 00
ELLIPTICITY		1.526E 00
CROSS AREA	(M**2)	1.061E 01
VOLUME	(M**3)	4.124E 02
TOROIDAL BETA	(MHD)	3.250E-02
POLOIDAL BETA	(MHD)	2.372E 00
POLOIDAL BETA	(AREA)	1.676E 00
POLOIDAL BETA	(VOLUME)	1.721E 00
Q-VALUE	(MHD)	3.942E 00
BV-SHAFRANOV	(T)	-4.871E-01
BV-CALCULATED	(T)	-4.415E-01
SUPPLIED FLUX	(WB)	1.106E-04
ABS TOTAL AMP	(AT)	1.108E 08
STORED ENERGY	(J)	1.336E 10
AMP-T METER	(AT-M)	3.974E 09
LIMITER R	(M)	5.610E 00
Z	(M)	-2.744E 00
PSI	(WB)	1.443E 01
RP (95%)	(M)	6.318E 00
AP (95%)	(M)	1.438E 00
ZP (95%)	(M)	1.999E-01
ELON-UPPER	(95%)	1.363E 00
ELON-LOWER	(95%)	1.760E 00
TRIANG-UPPER	(95%)	2.719E-01
TRIANG-LOWER	(95%)	4.036E-01

Fig. 3.4 (2) OTR plasma equilibrium calculation

INTOR SCOPING STUDIES

OTR SIMULATION

TIME = 1.000E 00 SEC

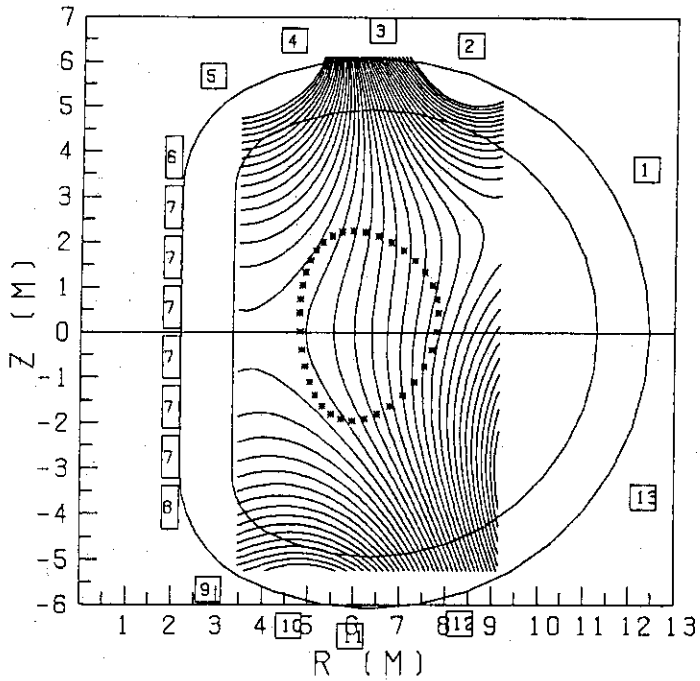

MIN=-2.000E 01
MAX= 1.900E 01
DEL= 1.000E 00

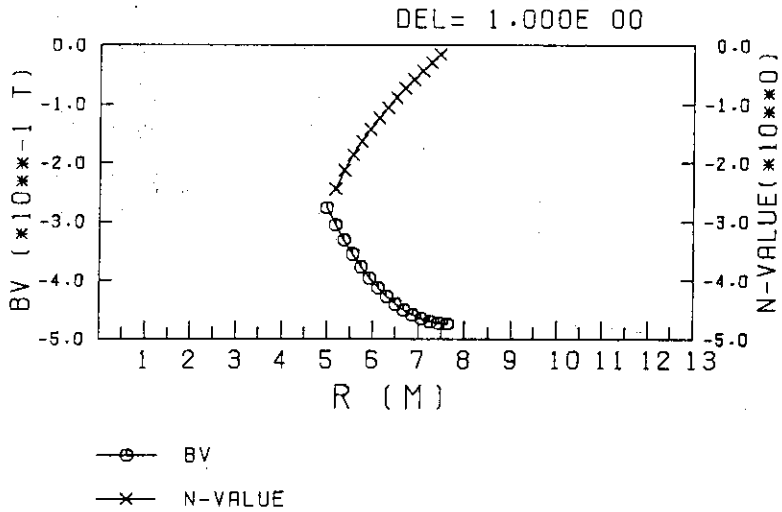

***** COILS **********

NO.	CURRENT(A)	BV(T)
1	6.176E 06	3.042E-01
2	-1.016E 07	-2.780E-01
3	-6.777E 06	-1.119E-01
4	1.641E 07	1.256E-01
5	1.617E 07	3.424E-02
6	8.522E 06	-4.051E-03
7	8.750E 05	-1.988E-02
8	3.853E 06	2.166E-04
9	8.613E 06	1.985E-02
10	8.234E 06	5.995E-02
11	7.211E 06	9.018E-02
12	-8.861E 04	-2.134E-03
13	-1.330E 07	-6.184E-01

Fig. 3.4 (3) OTR external field calculation

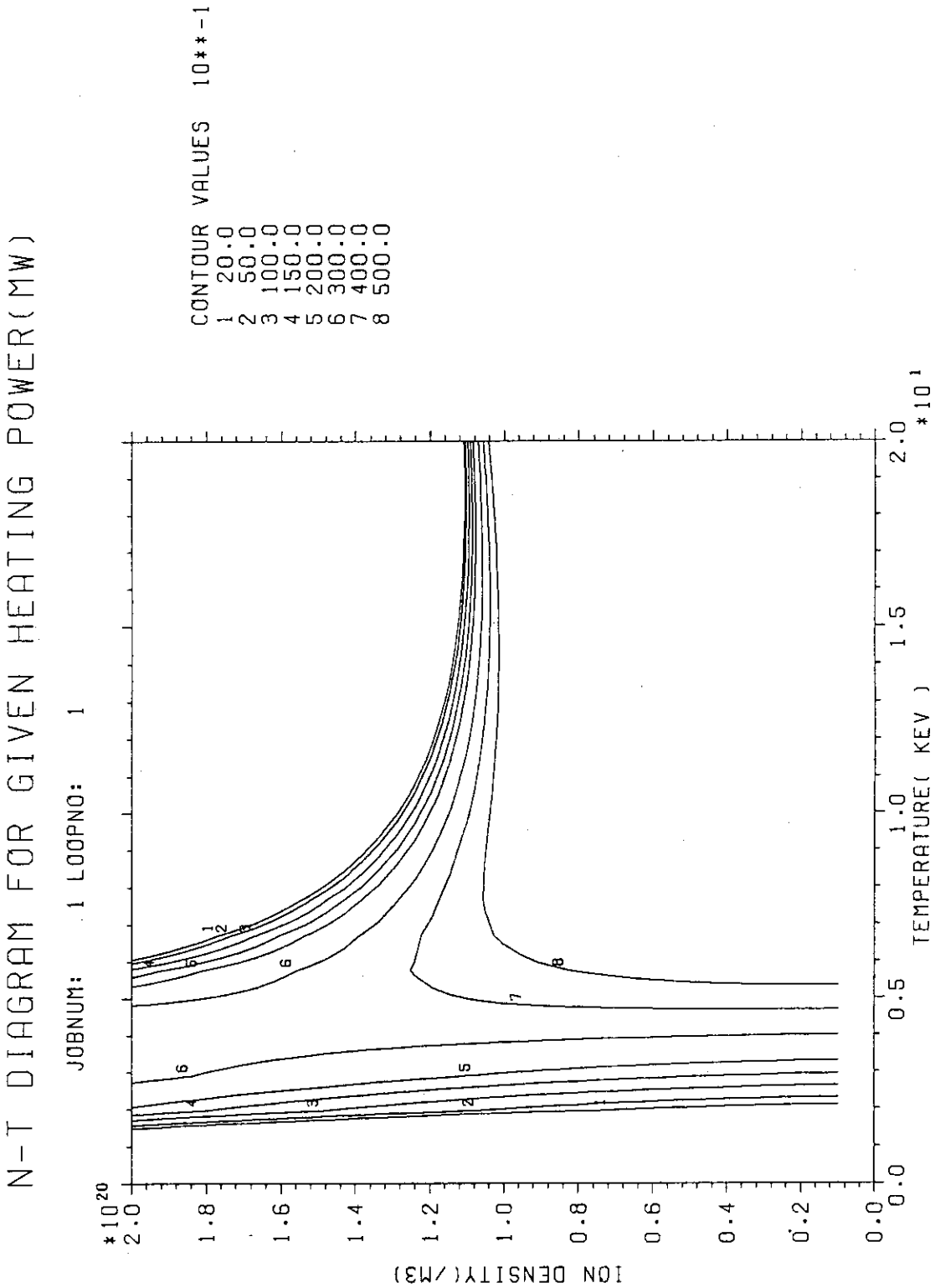

Fig. 3.4 (4) OTR plasma n-T diagram

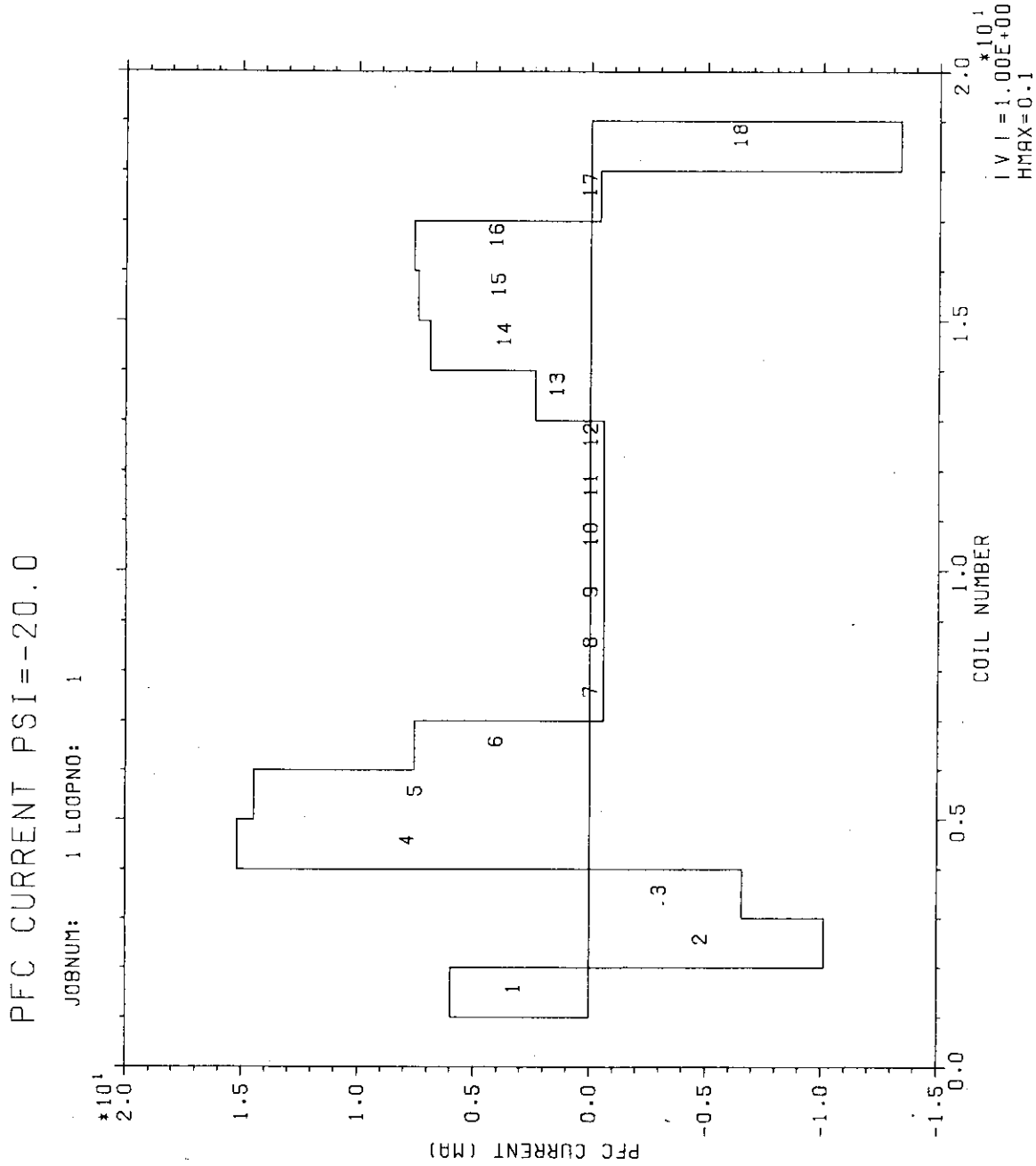

Fig. 3.4 (5) OTR PF coil current pattern at Ψ_p = -20 v.s

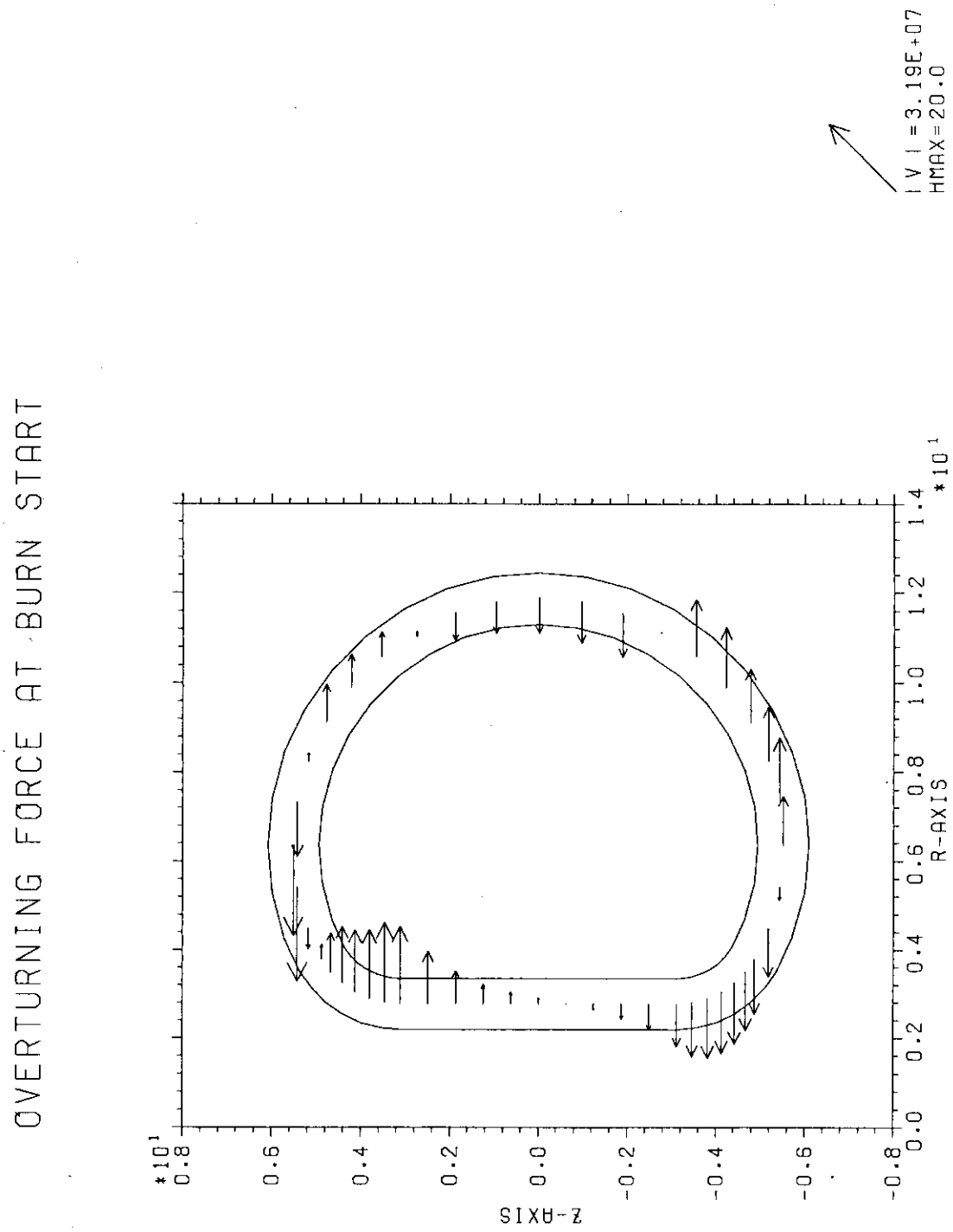

Fig. 3.4 (6) OTR overturning force on TFC

INTOR SCOPING STUDIES

OTR SIMULATION

TIME = 1.000E 00 SEC

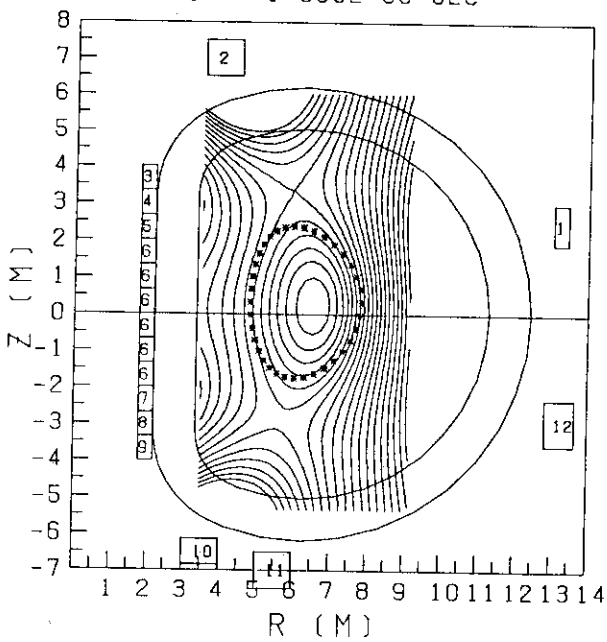

MIN= 1.294E 00
MAX= 1.929E 01
DEL= 1.000E 00

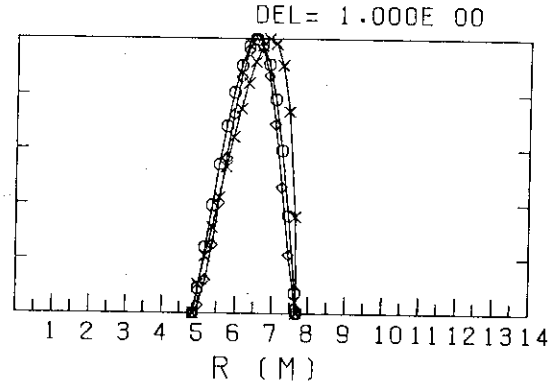

MAG.FLUX MAX= 2.005E 01.SURFACE= 1.429E 01

CUR.DENST. MAX= 1.352E 06 A/M**2

PRESSUR MAX= 1.247E 06 N/M**2

***** PLASMA PARAMETERS *********

IP-CURRENT	(A)	8.011E 06
VLOOP-SURFACE	(V)	-8.981E 01
SELF INDUCTANCE	(H)	1.376E-05
SMALL LI		8.769E-01
R-AVERAGE	(M)	6.268E 00
R-INNER	(M)	4.859E 00
R-OUTER	(M)	7.678E 00
R-MAGNETIC AXIS	(M)	6.512E 00
R-CURRENT MAX.	(M)	6.890E 00
A-HALF WIDTH	(M)	1.410E 00
A-AVERAGE	(M)	1.928E 00
ELLIPTICITY		1.871E 00
CROSS AREA	(M**2)	1.168E 01
VOLUME	(M**3)	4.572E 02
TOROLDAL BETA	(MHD)	3.250E-02
POLOIDAL BETA	(MHD)	3.265E 00
POLOIDAL BETA	(AREA)	2.012E 00
POLOIDAL BETA	(VOLUME)	2.056E 00
Q-VALUE	(MHD)	5.095E 00
BV-SHAFRANOV	(T)	-5.224E-01
BV-CALCULATED	(T)	-4.706E-01
SUPPLIED FLUX	(WB)	1.172E-04
ABS TOTAL AMP	(AT)	1.142E 08
STORED ENERGY	(J)	1.096E 10
AMP-T METER	(AT-M)	2.947E 09
LIMITER R	(M)	5.923E 00
Z	(M)	3.305E 00
PSI	(WB)	1.429E 01
RP (95%)	(M)	6.285E 00
AP (95%)	(M)	1.361E 00
ZP (95%)	(M)	2.269E-01
ELON-UPPER	(95%)	1.977E 00
ELON-LOWER	(95%)	1.914E 00
TRIANG-UPPER	(95%)	1.243E-01
TRIANG-LOWER	(95%)	2.634E-01

Fig. 3.4 (7) OTR plasma equilibrium with original PFC locations

4. Sensitivity Analysis

4.1 Guidelines

The critical analysis of INTOR-like designs was implemented in the engineering group task at the session XIV on December 1986. The purpose of this task is to clarify the reason why the INTOR-like designs differ from each other. The results of this analysis is expected to give useful database for discussing ITER design concept. The analysis is conducted in two ways, that is, global and individual sensitivity analyses. Since some design options are closely related, for example plasma elongation and selection of single or double null divertor, comparison of sets of certain design options gives us realistic effect on the machine design. We mainly examine those effects between INTOR and FER, and between NET and FER by substituting each physics, engineering and feature/driven constraints.

On the other hand, in order to have more clear individual effect, sensitivity of single design option based on its own machine design by each country has been added at the last session.

Japanese sensitivity analysis has been performed using the TRESCODE which was developed at JAERI for effective study of conceptual design of tokamak machine.

4.2 Global Sensitivities

4.2.1 Procedure of the analysis

The INTOR and NET designs are compared with FER design to clarify global sensitivities of the design constraints and features (drivers). Before the comparative procedure is conducted, the NET and INTOR designs are reproduced by the TRESCODE in order to confirm the consistency of each deligations design tools. The results are described at the top of the next section 4.2.2. Tables 4.1~4.5 show the procedure employed in comparison of NET and FER. Starting from the NET design, physics constraints are replaced with those of FER as a first step (Step A) and new machine parameters and relative cost are calculated. This step is devided into two substeps, namely, Step A-1 and A-2. In the Step A-1, inboard radial build is not changed although the required magnetic flux is reduced as a indirect effect of replacing physics design constraints in order to see the direct effect on plasma size. The indirect effect is included in the Step A-2 which shows total effect of physics constraints difference. The engineering constraints (Step B) and features (Step C) are replaced with those of FER. The Step C has been done agin with two substeps. At the first substep some of features, which is expected to increase machine dimensions by the substitution, are replaced. Rest of the features are replaced at the second substep decreasing reactor dimensions. Comparative study between INTOR and FER is conducted in the same steps as the above except that the A-1 and A-2 are combined because the required magnetic flux scarcely changed by the substitution of the physics constraints. The design features of the INTOR, NET and FER are summarized in Table 4.6. In the above procedures, missions of each machine are substituted not explicity but implicitly when constraints and features are replaced.

4.2.2 Simulation of INTOR and NET plasmas

In a starting point of comparative studies, the differences in the Physics are examined and summarized in Table 4.7. There is some confusion between plasma specifications and the Physics in INTOR design. For example, the ratio of β and β_{DT} should be 1.19 according to the specifications, byt 1.28 (at 10 keV) in the Physics constraints. The elongation of 1.6 described at both specifications and Physics constraints is not the averaged elongation but the elongation at the non-null point side (or upper side) according to a plasma configuration figure. The averaged elongation should be about 1.75 on the surface defined by 95% of ψ_p. Nevertheless, we try to simulate the INTOR plasma using the INTOR Physics shown in Table 4.7 and the results are shown in Table 4.8. Here, the plasma size, shape, current and toroidal field on axis are exactely simulated with adjusting a safety factor q and ignition margin I_g. Similary, the NET plasma is also reproduced by introducing the NET Physics described in Table 4.7. The results is also shown in Table 4.8. One of the difficulties to simulate the NET plasma is resulted from different definitions of the safety factor q_I and plasma non-circularity.

We investigate ignition margins for three devices to use different types of definition. The summary is shown in Table 4.9. The ignition margin, $I_g^{(1)}$, is defined by the ratio of the alpha heating power and the total loss power including the convection power loss of ion and electron and radiation losses. However, by the another definition the ignition margin, $I_g^{(2)}$, is defined as the ratio of the alpha heating power and the convection power loss due to fuel plasma. INTOR and NETDN plasmas holds the ignition margin, $I_g^{(2)}$, of three. However, using the former definition, $I_g^{(1)}$, those of INTOR and NETDN are 0.9 and 1.0 respectively. The aspect ratio of INTOR is 4.2. In this case of large aspect ratio, the ASDEX-H type scaling may overestimate the confinement time and the Mirnov type scaling may underestimate the confinement time. This is why $I_g^{(1)}$=0.9 in spite of $I_g^{(2)}$=3.0. In NET, on the other hand, $I_g^{(2)}$ is calculated to be 3.0 without considering radiation power loss. This is a little tricky. According to the NET Physics constraints, Z_{eff}=2.0 and β/β_{DT}=1.34 so that $n_e=1.7\times10^{19}$ m^{-3}. Then the radiation power loss due to bremsstrahlung is 32 MW and synchrotron is 8 MW. The

total radiation power loss is about 30% of the alpha heating power. This is main reason why $I_g^{(1)}$=1.0 in spite of $I_g^{(2)}$=3.0 in NET. It can say that confinement capability both of NET and FER is almost same under FER power balance considerations. Differences on plasma parameters may come from different physics constraints such as n_e/n_{DT}, β/β_{DT} and q.

4.2.3 Comparative study results between INTOR and FER

(1) Impact on the radial build in Step A

The toroidal beta reduces because of changing the coefficient of the Troyon scaling to 3.5 from 4.0. But the plasma current tends to increase because of relatively lower q value in FER physics constraints. These effects compensate each other and the resultant plasma is quite similar to INTOR plasma, as shown in Table 4.10. Thus there is almost no impact on the INTOR design due to substituting of FER Physics for the INTOR Physics.

(2) Impact on the radial build in Step B

In the INTOR Engineering, maximum field of the solenoid coil is 8 T and the current density of superconductor is low. Substituting the FER Engineering of which the maximum field and the current density for the solenoids are 10 T and 30 A/mm² respectively, the end radius of the solenoid coils can reduce about 30 cm even the required volt second slightly increase. On the other hand, the maximum field of TFC B_{Tmax} in INTOR Engineering is 11 T, but the ripple effect α at the inner leg is assumed only 1.04, undoutedly low. In the FER Engineering, B_{Tmax}=12T but α=1.2 so that the useful field B_{max} (=B_{Tmax}/α) is 10 T. As a result, the toroidal field on the plasma axis tends to be smaller. This is the reason why the plasma minor radius increase about 8 cm in Step B. Comparison on radial-build is shown in Fig. 4.1. The shield thickness shows no change. The thermal shield thickness reduces from 0.15 m to 0.085 m. In conclusion, the impact on the INTOR in Step B is reduction of the plasma major radius from 4.99 m to 4.76 m. Main contribution for that come from the solenoid coil design conditions.

(3) Impact on the radial build in Step C

Some of design features in Physics and Engineering for INTOR is the similar to those for FER design. As discussed before, Step C is devided in two substeps. In the first substep, Step C-1, we substitute the FER

plasma shape for the INTOR plasma shape. Both shapes are quite similar with single null divertor so that there is no big impact in this step. In the second substep, Step C2, the reduction of the designed volt second due to hybrid operation scenario, the reduction of the life time fluence and shield blanket without T-breeding are introduced as the FER design features. As a result, FER device is obtained. Impact on the major radius are the following;

i) Reduction of the designed volt second due to non inductive current ramp ==

end radius of the solenoid → -0.25 m

ii) Reduction of the total fluence ==

shield thickness → -0.085 m

plasma minor radius → -0.06 m

(4) Impacts on machine cost

Because of smaller size of machine. Some cost reduction are expected for FER on the reactor structure and assembly, magnet, especially TFC, and power supply system. The preliminary results of cost estimation shows that the cost of the INTOR device is about 16% higher than that of the FER device.

4.2.4 Comparative study results between NET and FER

(1) Impact on the radial build in Step A

In the calculation of the Step A-1, inboard radial build is not changed in order to keep NET engineering constraints unchanged. Then some effects on the OH coil dimension due to the change of plasma parameters, for example, plasma current, is not included. The plasma minor radius decreases by -24 cm by replacing NET Physics with FER Physics as shown in Table 4.11. There are two reasons for that. At first, the fraction of fuel density in FER Physics is higher than that of FER Physics. Hence, the fusion power density is higher and radiation loss is smaller in FER Physics. Second, the safety factor is relatively lower in FER Physics. These two physics constraints allows to make smaller plasma. As a results, the plasma current can reduce to 8.5 MA. In a different point of view, if the plasma size and noncircularity could be held as same as the NET plasma and FER Physics applied, then the NET plasma would have the ignition margin, $I_g^{(1)}$, of 1.7.

In the Step A-2, further reduction of plasma major radius is obtained. As discussed in the above, the plasma current can be reduced with FER Physics. Using the Ejima's empirical formula for the required magnetic flux during full inductive current ramp-up, $\Delta\phi = L_p^{ex} I_p + 1.35R\ I_p$ magnetic flux with the burn time of 350 sec should be 143 volt second with the reduced plasma current of 8.7 MA. Because of this reduction the end radius of the solenoid coils become 1.45 m, about 0.3 m less than NET design.

(2) Impact on the radial build in Step B

Slight impacts come from the reduction of the plasma scrape-off layer and TF coil design constraints such as the ripple effect at the inner leg of TFC. Total impacts are the following, as shown in Fig. 4.2,

i) less scrape-off layer == $\Delta_{s,o}$ → -0.1 m

ii) TFC design constraints == a → +0.03 m.

Thus FER Physics associated with FER engineering can produce about 0.6 m smaller plasma than original NET plasma.

(3) Impact on the NET design in Step C

At the Step C-1, four features are replaced which increase reactor size. Plasma elongation is changed to 1.7 from 2.2 and double null divertor configuration is substituted with the single null. Wedging support of centering froce of TF coil is changed to the bucking cylinber support. Those replacements increase plasma major radius by -90 cm in total. The other changes, number of TF coil and maintenance approach do not change the plasma major radius but have effect on the outer leg position of TF coil. At the step C-2 three features are replaced which decreases plasma radius. They are operation mode, life time fluence and T-breeding capability. Those replacements reduce plasma major radius about 1 m in total leading to the exactly same radial dimensions as FER finally. Combination effect of the reducing life time fluence and eliminating T-breeding blanket corresponded to the 50 cm reduction and other half comes from the solenoid coil bore reduction due to the operational mode change.

So impacts on the major radius in Step C-1 are summalized as follows,

(i) change plasma elongation == a → +0.28 m

(ii) scrape-off layer for SND == $\Delta_{s,o}$ → +0.13 m

(iii) bucking cylinder support == $\Delta_{B,C}$ → +0.23 m

(iv) increase of the required flux == Δ_{OH} → +0.25 m

Total increase +0.89 m

In Step C-2

(i) choice of non-inductive current ramp-up == R_{OH} → -0.52

(ii) no T-breeding blanket == Δ_{BLKT} → -0.36

(iii) reduce life-time fluence == Δ_{SLD} a → -0.17

Total reduction -1.05

(4) Impacts on the machine cost

Impacts on the machine cost are shown in Fig. 4.3. This figure shows the relative cost in each step. As explained above the change from "NET" to "Step A-2" can be taken as physics constraints effect and it correspond to the -11% reduction of cost. Then if we reduce elongantion to 1.7, and employ bucking cyclinder support for TFC the cost increase -11%. Then elimination of T-breeding blanket and reducing lifetime fluence and emplyment of non-inductive current drive operation reduce reactor cost -27%.

Table 4.1 Step A-1 Substitute the FER physics for the NET physics

EC NET/DN	Japan FER
NET mission	FER mission
NET features	FER features
FER physics ←	FER physics
NET engineering	FER engineering

(1) Fix inner torus radial-build --- NET engineerings
(2) Keep NET plasma shape --- NET features

Table 4.2 Step A-2 Substitute the FER physics for the NET physics

EC NET/DN	Japan FER
NET mission	FER mission
NET Features	FER features
FER physics —	FER physics
NET engineering	FER engineering

(1) Change designed volt·sec but
Keep full inductive ramp up --- NET features
(2) Keep Magnet design condition --- NET engineering
(3) Keep NET plasma shape --- NET features

Table 4.3 Step B Substitute the FER physics and engineerings for the NET physics and engineerings

EC NET/DN		Japan FER
NET mission		FER mission
NET features		FER features
FER physics	←	FER physics
FER engineerings	←	FER engineering

(1) Keep NET plasma shape ——— NET features
(2) Keep full inductive operation —— NET features
(3) Keep life time fluence ——— NET features
(4) Keep blanket ——— NET features
(5) Keep vertical access ——— NET features
(6) Keep wedge support ——— NET features

Table 4.4 Step C-1 Substitute the FER Physics, engineerings & some features for the NET Physics, engineerings & some features

EC NET/DN		Japan FER
NET mission		FER mission
FER features	←- - -	FER features
FER physics	←	FER features
FER engineering	←	FER engineering

Changed some features

(1) Plasma shape, DN → SN
(2) Wedge support → Bucking Cylinder
(3) Number of TFC → 16 → 12
(4) Vertical access → Horizontal access

Kept other features

(1) Full inductive operation
(2) Life time fluence
(3) Blanket → Shield blanket

Table 4.5 Step C-2 Substitute the FER Physics, engineering & all features for the NET Physics, engineering & all features

EC NET/DN		Japan FER
NET mission		FER mission
FER features	←	FER features
FER physics	←	FER features
FER engineering	←	FER engineering

Table 4.6 Difference of Design Drivers (Features)

	INTOR	NET	FER
1) Plasma Shspe			
Divertor	SN	DN	SN
κ		2.2	1.7
δ		0.65	0.2
2) Operation Mode	full inductive	full inductive	non-inductive ramp-up
3) Fluence	3 MWY/m^2	3 MWY/m^2 (0.8)	0.3 MWY/m^2
4) Blanket	T-breeding blanket	T-breeding blanket	Shield
5) Maintenance	Horizontal	Vertical	Horizontal
6) TF Support	Not specified (Bucking cylinder)	Wedge	Bucking cylinder
7) Number of TFC	12	16	12

Table 4.7 Comparison of NET, INTOR, FER, TIBER and OTR physics

Items	NET	FER	INTOR	TIBER	OTR
Power balance (for self-ignition)	$\frac{3\,k n_{DT} T}{\tau_E} = \frac{1.5\times10^6\ \beta_{DT}^2 B_T^4}{I_g} \frac{E_\alpha}{E_f}$ $I_g \equiv \frac{P_\alpha}{P_{loss}}$ $P_{loo} = \frac{3\,k n_{DT} T}{\tau_E}$	$\frac{\frac{3}{2} k(n_e+n_i)T}{\tau_E} + P_{br} + P_{sy}$ $= f_T\, n_D n_T \langle\sigma v\rangle E_\alpha(1+\frac{5}{Q})$ $f_T = 1.5$ $Q \geq 20$	$\frac{3\,k n_{DT} T}{\tau_E} = \frac{1.5\times10^6\ \beta_{DT}^2 B_T^4}{I_g} \frac{E_\alpha}{E_f}$ $I_g \equiv \frac{P_\alpha}{P_{loss}}$ $P_{loss} = \frac{3\,k n_{DT} T}{\tau_E}$	$\frac{\frac{3}{2} k(n_e T_e + n_i T_i)}{\tau_E}$ $=1.5\ n_D\, n_T \langle\sigma v\rangle E_\alpha(1+\frac{5}{Q})$ $Q \geq 5$	
Confinement time scaling law	ASDEX-H $\tau_E^{NET} = 0.065\ R\ I_p \sqrt{M}$ (m)(MA) $M = 2.5$ with $I_g^{NET} = 2.9$	Mirnov-type $\tau_E^{FER} = 0.155\ a\ I_p \sqrt{\kappa}$ (m)(MA)	ASDEX-H $\tau_E = 0.12\ R\ I_p$ (m)(MA) $I_g \sim 3.0$	Kaye-Goldston [4] $\tau_E = H \times \tau_E^{KG}$	T-11 [4]
Beta scaling law	Troyon scaling $\beta(\%) = G \frac{I_p(MA)}{a(m)\ B_T(T)}$ $G = 3.5$	Troyon scaling $\beta(\%) = G \frac{I_p(MA)}{a(m)\ B_T(T)}$ $G = 3.5$	Troyon scaling $\beta(\%) = G \frac{I_p(MA)}{a(m)\ B_T(m)}$ $G \sim 4.0$	Troyon scaling $\beta(\%) = G \frac{I_p(MA)}{a(m)\ B_T(m)}$ $G \sim 3.0$ or Yamazaki scaling	Troyon scaling $\beta(\%) = G \frac{I_p(MA)}{a(m)\ B_T(m)}$ $G = 3.5$

Table 4.7 (Continued)

Items	NET	FER	INTOR	TIBER	OTR
Ion composition	n_{He} = 8% + (i) n_{imp} (C,O) = 2% (ii) n_{imp} (medium Z) = 0.05% (iii) n_{imp} (high Z) = 0.005% Remains are $n_D + n_T$ ⇓ Z_{eff} = 2.0, n_e/n_{DT} = 1.34	n_{He} = 5% + $n_C = n_O$ = 0.5% n_H = 1% $n_D = n_T$ = 46.5% ⇓ Z_{eff} = 1.5, n_e/n_{DT} = 1.23	n_{ne} = 5% $n_C = n_O$ = 0.5% $n_D = n_T$ = 47% ⇓ Z_{eff} = 1.5	n_{He} = 5% n_O = 0.24% $n_D = n_T$ = 47.38% ⇓ Z_{eff} = 1.5	n_{He} = 5% n_H = 1% $n_C + n_O$ ~ 1% $n_D = n_T$ = 46.5% ⇓ Z_{eff} = 1.5
Fuel beta	β / β_{DT} = 1.34 fast α pressure = 10%	β / β_{DT} = 1.23 fast α pressure = 8% at 12 keV (5% at 10 keV)	β / β_{DT} = 1.19 fast α = 7 % at 10 keV	β / β_{DT} = 1.6 fast α pressure ?	β / β_{DT} = 1.2
Safety factor	$q_I = \frac{5a^2 B_T}{R I_p(MA)} K^2$ $K = \oint \frac{dl_p}{2\pi a}$ Surface for line integration: $R = R_p + a\cos(\theta + \delta_N \sin)$ $Z = \kappa_N a \sin\theta$ κ_N, δ_N are the noncircularity at the separatrix.	$q_\psi = \frac{5a^2 B_T}{R I_p(MA)} f(\kappa,\delta)$ $f(\kappa,\delta) = \frac{1+\kappa^2}{2}\left(1 + \frac{0.16+0.633\delta}{\sqrt{A}}\right) \times \left(1 + \frac{\beta_p(0.45+\delta)}{A^{1.5}}\right)$ κ, δ are the noncircularity at the surface defined by 95% ψ_p.	$q_I = \frac{5a^2 B_T}{R I_p(MA)} \frac{1+\kappa^2}{2}$ κ is the plasma average elongation at the surface defined by 95% ψ_p.	$q_I = \frac{5a^2 B_T}{R I_p(MA)} \frac{1+\kappa^2}{2}$ κ is the plasma average elongation at the surface defined by 95% ψ_p.	$q_I = \frac{5a^2 B_T}{R I_p(MA)} \frac{1+\kappa^2}{2}$ κ is the plasma average elongation at the surface defined by 95% ψ_p.

Table 4.8 Plasma Major Parameters of NET,FER and INTOR

	NET	FER	INTOR
Plasma major madius	5.18 m	4.42 m	5.0 m
Plasma minor madius	1.35 m	1.25 m	1.2 m
Aspect ratio	3.83	3.54	4.17
Plasma elongation	2.18 at null	$\tilde{\kappa}$ = 1.7 SND	$\tilde{\kappa}$ = 1.75 SND
Plasma triangularity	0.65 at null	$\tilde{\delta}$ = 0.2 SND	$\tilde{\delta}$ = 0.2 SND
Plasma current	10.8 MA	8.7 MA	8.0 MA
Toroidal field on axis	5.0 T	4.6 T	5.5 T
Safety factor	2.24 (1)	2.6 (2)	2.0 (3)
Toroidal beta	5.6 %	5.3 %	4.9 %
Fuel beta	4.2 %	4.3 %	4.1 %
Electron density	1.7×10^{20}	1.1×10^{20}	1.8×10^{20}
Ion density	1.4×10^{20}	1.0×10^{20}	1.6×10^{20}
Fuel density	1.3×10^{20}	0.96×10^{20}	1.5×10^{20}
Z_{eff}	1.9 (3')	1.5	1.5
Plasma volume	409 M^3 (4)	230 M^3 (5)	249 M^3 (5)
Fusion power	661 MW	404 MW	558 MW
Alpha power	133 MW	81 MW	112 MW
Bremsstrahlung	(32 MW)	7 MW	17 MW
Synchrotron radiation	(8 MW)	5 MW	7 MW
Neutron wall load	1.1 MW/m^2	1.1 MW/m^2	1.3 MW/m^2
Maximum field	11.4 T	12 T	11.7 T
Required volt. sec	(181 v.s)	85 v.s	(130 v.s)

(1) $q_I = \frac{5a^2 B_T}{R I_p(MA)} K^2$ $\qquad K = \int \frac{d\ell_p}{2\pi a}$

(2) $q_\psi = \frac{5a^2 B_T}{R I_p(MA)} f(\kappa,\sigma,A)$ $\qquad$ (3) $q_I = \frac{5a^2 B_T}{R I_p(MA)} \frac{1+\tilde{\kappa}^2}{2}$

(3') n_{He} = 8 %, $n_c = n_o$ = 1.0 %, $n_D = n_T$ = 45.0 %,

(4) Vol = $2\pi^2 \kappa_N a^2 R$ $\qquad \kappa_N$ at separatrix

(5) Vol = $2\pi^2 \tilde{\kappa} a^2 R$ $\qquad \kappa$ at ψ_{95}

Table 4.9 The assessment of the ignition margin for FER, NET and INTER

		FER	NET	INTOR
$I_G^{(1)}$	MIRNOV-TYPE	1.0	1.0	0.9
	ASDEX-H	1.7	1.4	1.7
$I_G^{(2)}$	MIRNOV-TYPE	1.4	1.7	1.2
	ASDEX-H	2.5	3.0	3.0

$$I_G^{(1)} = \frac{P_\alpha}{1.5\ (N_e + N_i)kTVo\ell\ /\ \tau_E + P_{br} + P_{sy}}$$

$$I_G^{(2)} = \frac{P_\alpha}{3.0n_{DT}kTVo\ell\ /\ \tau_E}$$

$$\tau_E^{Mirnov} = 0.155\ a\ I_p\ (MA)\ \sqrt{\kappa}$$

$$\tau_E^{ASDEX-H} = 0.065\ R\ I_p\ (MA)\ \sqrt{M}$$

$$\tau_E^{ASDEX-H}\ (INTOR) = 0.12\ R\ I_p\ (MA)$$

Table 4.10 Plasma Parameters (INTOR/FER)

	INTOR	Step A	Step B	Step C-1	FER (Step C-2)
Plasma major madius	5.0 m	4.99 m	4.76 m	4.81 m	4.42 m
Plasma minor madius	1.2 m	1.19 m	1.27 m	1.31 m	1.25 m
Aspect ratio	4.17	4.2	3.75	3.68	3.54
Plasma elongation	$\kappa_u = 1.6$ $\tilde{\kappa} = 1.75$	←	←	$\tilde{\kappa} = 1.7$ at ψ_{95} SND	←
Plasma triangularity	$\tilde{\delta} = 0.2$	←	←	$\tilde{\delta} = 0.2$ at ψ_{95} SND	←
Plasma current	8.0 MA	8.3 MA	8.8 MA	8.9 MA	8.7 MA
Toroidal field on axis	5.5 T	5.5 T	4.8 T	4.8 T	4.6 T
Safety factor	2.01(1)	2.6(2)	←	←	←
Toroidal beta	4.8 % (G=4.0)	4.4 %	5.1 %	5.0 %	5.3 %
Fuel beta	4.0 %	3.6 %	4.1 %	4.1 %	4.3 %
Electron density ($\times 10^{20}$)	1.79	1.35	1.18	1.14	1.14
Ion density ($\times 10^{20}$)	1.61	1.22	1.06	1.03	1.03
Fuel density ($\times 10^{20}$)	1.50	1.13	0.99	0.96	0.96
Z_{eff}	1.5	1.5	1.5	1.5	1.5
Plasma volume	250 M^3(4)	243 M^3(5)	263 M^3(5)	276 M^3(5)	230(5)
Fusion power	557 MW	538 MW	445 MW	440 MW	404
Alpha power	111 MW	108 MW	89 MW	88 MW	81
Bremsstrahlung	17 MW	10 MW	8 MW	8 MW	7
Synchrotron radiation	7 MW	8 MW	6 MW	6 MW	5
Neutron wall load	1.3 MW/m^2	1.3 MW/m^2	1.0 MW/m^2	1.0 MW/m^2	1.1
Maximum toroidal field	11.0 T/1.04	←	12.0 T/1.20	←	←
Required volt. sec	130 v.s	134 v.s	138 v.s	139 v.s	85 v.s
Burn temperature	10 KeV	10 KeV	←	←	←
Burn time	200 sec	←	←	←	800 sec
Operation scenario	full ind.	←	←	←	hybrid

(1) $q_I = \frac{5a^2 B_T}{R I_p(MA)} K^2 \qquad K = \frac{1+\tilde{\kappa}^2}{2}$

(2) $q_\psi = \frac{5a^2 B_T}{R I_p(MA)} f(\kappa,\sigma,A)$

(3) $n_{He} = 8\ \%, \quad n_c = n_o = 1.0\ \%, \quad n_D = n_T = 45.0\ \%$

(4) $Vol = 2\pi^2 \kappa_N a^2 R \qquad \kappa_N$ at separatrix

(5) $Vol = 2\pi^2 \tilde{\kappa} a^2 R \qquad \kappa$ at ψ_{95}

Table 4.11 Plasma Parameter (NET/FER)

	NET	Step A	Step B	Step C-1	FER (Step C-2)
Plasma major madius	5.18 m	4.94 m	4.58 m	5.47 m	4.42 m
Plasma minor madius	1.35 m	1.11 m	1.14 m	1.42 m	1.25 m
Aspect ratio	3.83	4.46	4.00	3.86	3.54
Plasma elongatoin	2.18 at null	←	←	$\tilde{\kappa}$ = 1.7 at ψ_{95} SND	←
Plasma triangularity	0.65 at null	←	←	$\tilde{\delta}$ = 0.2 at ψ_{95} SND	←
Plasma current	10.8 MA	8.5 MA	8.9 MA	9.0 MA	8.7 MA
Toroidal field on axis	5.0 T	5.2 T	4.5 T	4.7 T	4.6 T
Safety factor	2.24(1)	2.6(2)	←	←	←
Toroidal beta	5.6 %	5.1 %	6.0 %	4.7 %	5.3 %
Fuel beta	4.2 %	4.2 %	4.9 %	3.9 %	4.3 %
Electron density ($\times 10^{20}$)	1.7	1.4	1.2	1.05	1.14
Ion density ($\times 10^{20}$)	1.4	1.3	1.1	0.75	1.03
Fuel density ($\times 10^{20}$)	1.3	1.2	1.0	0.88	0.96
Z_{eff}	1.9(3)	1.5	←	←	←
Plasma volume	409 M^3(4)	222 M^3(5)	220 M^3(5)	370(5)	230(5)
Fusion power	661 MW	544 MW	411 MW	495 MW	404
Alpha power	133 MW	109 MW	82 MW	99 MW	81
Bremsstrahlung	(32 MW)	10 MW	8 MW	9 MW	7
Synchrotron radiation	(8 MW)	7 MW	5 MW	7 MW	5
Neutron wall load	1.1 MW/m^2	1.4 MW/m^2	1.1 MW/m^2	0.9 MW/m^2	1.1
Maximum toroidal field	11.4 T/1.09	11.4 T/1.09	12 T/1.20	←	←
Required volt. sec	181 v.s	157 v.s	143	167	85
Burn temperature	12 KeV	10 KeV	←	←	←
Burn time	350 sec	←	←	←	800 sec
Operation scenario	full ind.	←	←	←	hy brid

(1) $q_I = \frac{5a^2 B_T}{R I_p(MA)} K^2 \qquad K = \int \frac{d\ell_p}{2\pi a}$

(2) $q_\psi = \frac{5a^2 B_T}{R I_p(MA)} f(\kappa,\sigma,A)$

(3) n_{He} = 8 %, $n_c = n_o$ = 1.0 %, $n_D = n_T$ = 45.0 %

(4) Vol = $2\pi^2 \kappa_N a^2 R$ $\quad \kappa_N$ at separatrix

(5) Vol = $2\pi^2 \tilde{\kappa} a^2 R$ $\quad \kappa$ at ψ_{95}

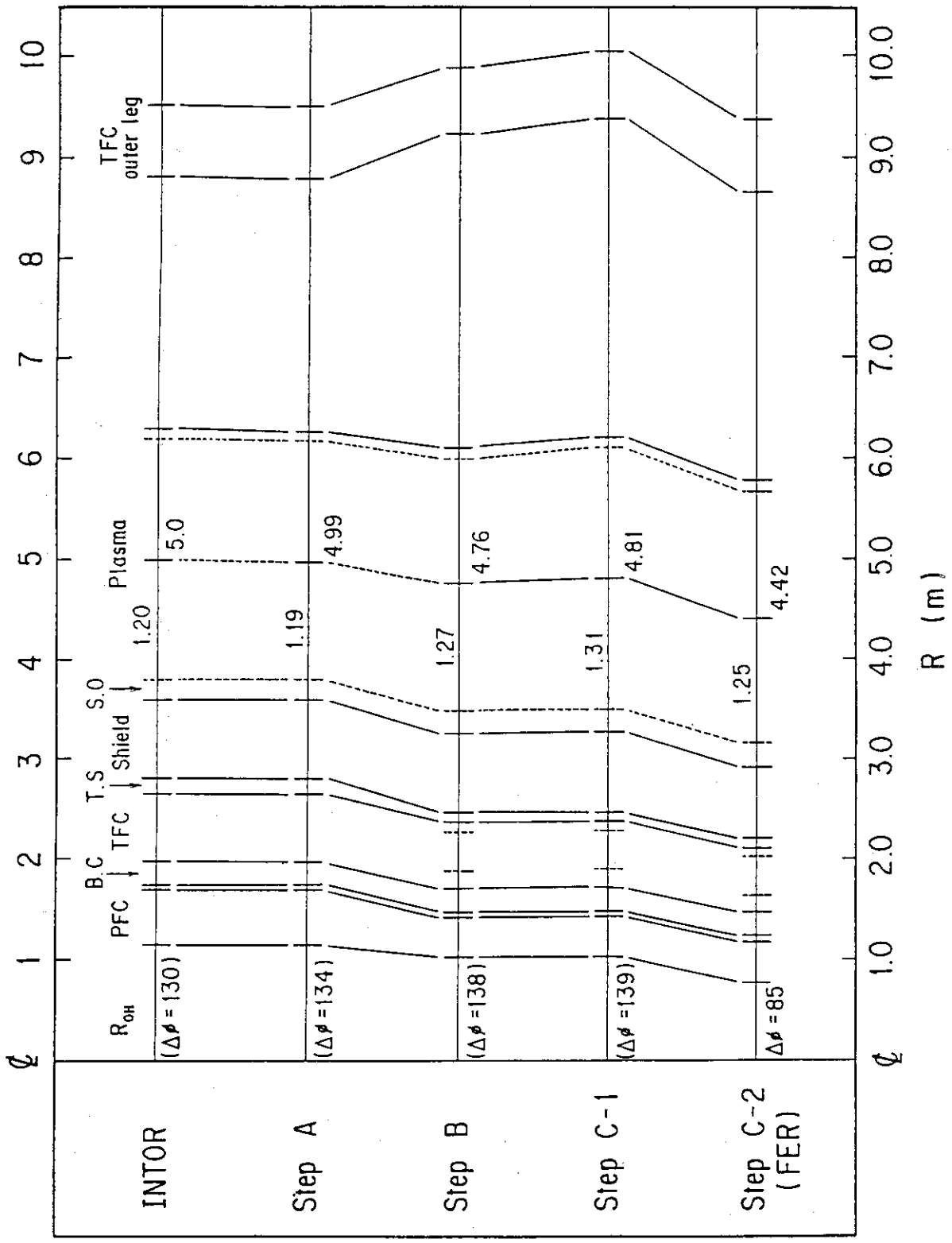

Fig. 4.1 Radial - build comparizon for INTOR and FER

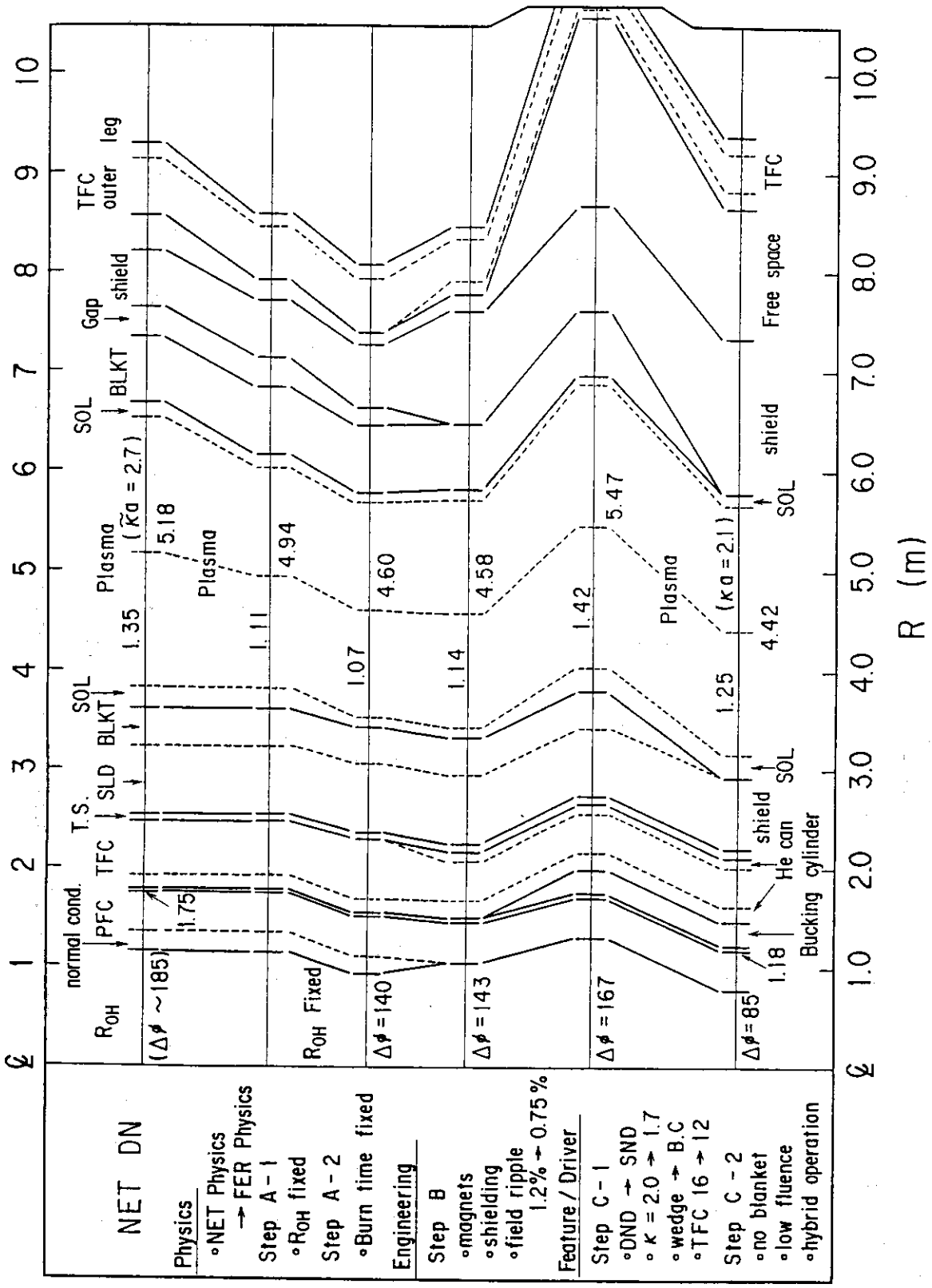

Fig. 4.2 Radial- build comparizon for NET and FER

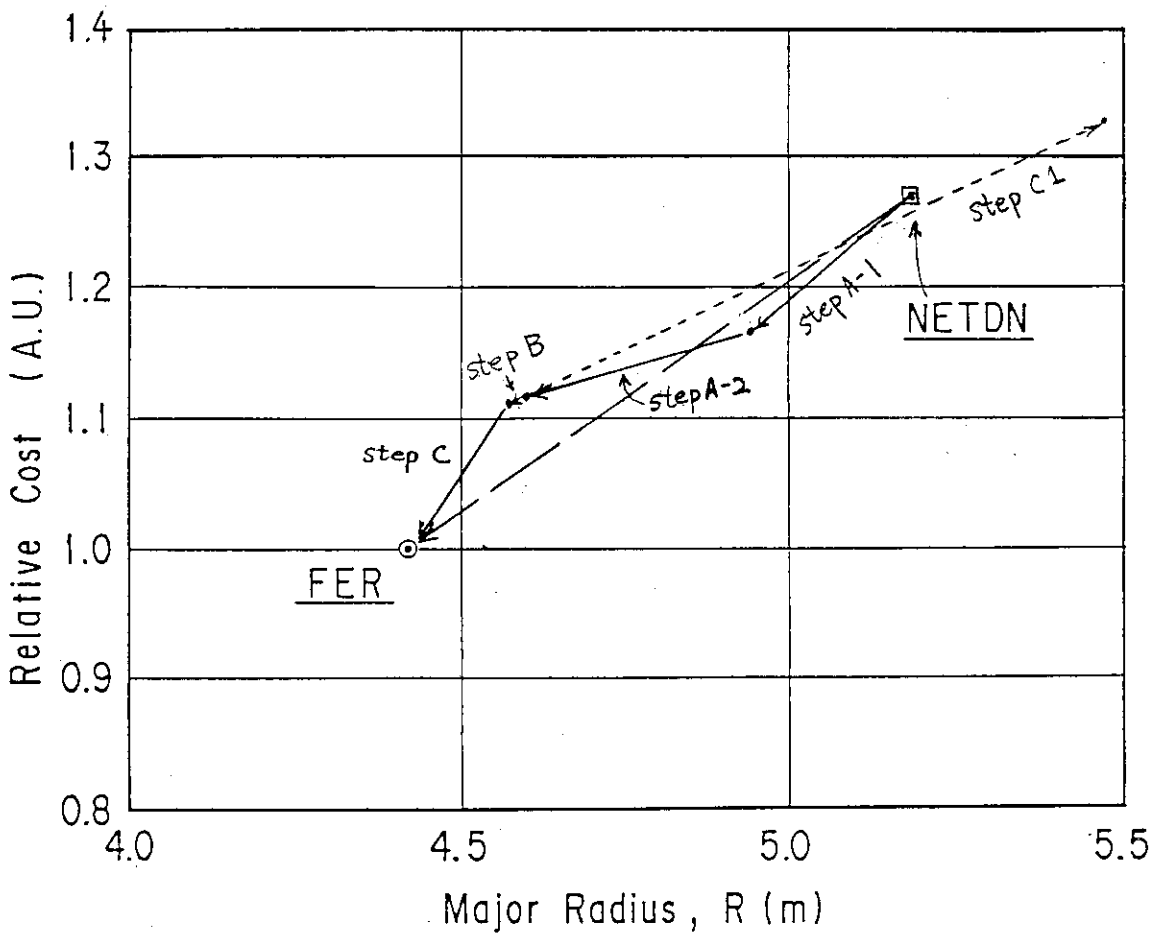

Fig. 4.3 Relative Cost of Each Step From NET to FER

4.3 Individual Sensitivities

At the last session, new sensitivity study was added as a home task of the group H in order to make this comparative study more detail. Since the global sensitivity analysis does not necessarily reveal the sensitivities of individual design options it is prefered to conduct some sensitivity analysis for the single change which is expected to give large impact on the machine design. In our analysis FER design is taken as a base machine according to the guideline. Machine parameters and assumptions are shown in Table 4.12. Mirnor type scaling law is used for the energy confinement time. The eight design options are listed in Table 4.13 with their ranges and impacts on the plasma major radius and direct capital cost of the reactor. When one of the design options changed the rest options remaines same as selected in FER. The calculational results are shown also in Fig. 4.4-4.6. In the Rp-a plane the changes of ignition margin, Troyon coefficient, safety factor, plasma elongation and Z_{eff} give the machine dimensions on the single line as shown in Fig. 4.4 because the end radius of solenoid coils and other engineering radial-build are fixed. Magnetic flux capability gives big impact on the major radius but slight on minor radius. Increase of the peak field of TF magnet gives smaller plasma minor radius but not necessarily smaller major radius. Around 11.5 T the major radius become minimum. The above calculation about the maximum field change is conducted with the assumption of inversly decreasing average current density in conductor with the maximum field. Since neutron wall loading increases with the maximum field, the required thickness of the shield is also changed. The more detailed calculation with constant tensile stress in TFC inboard leg is also conducted and the results are shown in Fig. 4.5. From this figure this effect seems to be not large. However, it is noted that the risk of having higher bending stress in the side wall of TF coil case possiblly increase. Figure 4.5 also shows a case with constant shielding thickness case. In this case the minimum plasma major radius appears around 13 T. As shown in Fig. 4.6 the capital cost of the reactor alway increase with the plasma major radius except the case of chainging the TFC maximum field around 11T. Then the plasma major radius is the one of the good

indicator for the capital cost. However, the individual sensitivities for the capital cost are different. For example, if the plasma holds larger ignition margin, that means not only an increase of plasma size but also an increase of fusion power output due to the power balance requirement. Fusion power enhancement results in an increase of plasma current. Larger plasma current requires higher cost for magnet systems. Large fusion power also requires a cost-up for cooling systems. Thus we have to pay for also of this and the sensitivity of Ignition margin to the cost become very large. For the case of heigher magnetic field, increase of the major radius is caused by mainly thicker TF coil that means signiticant increase of the cost. In addition fusion power increases proportionally to B_T^4 leading to the further cost increase. Then the sensitivity of the higher magnetic field is even larger than that of the ignition margin. In a case of increasing Z_{eff}, fusion power also increases to compensate the power loss due to radiations. On the other hand, changing of q_ψ, G or κ does not mean increase of plasma current, thus fusion power doesn't increase significantly. As a results, cost sensitivity for these options is rather weak. Changing of disigned volt second affect greatly to plasma major radius but slightly to the plasma minor radius and other plasma parameters. The cost sensitivity of $\Delta\phi$ is thus weak. It is noted, however, that additional cost for electric power supply will be required if full inductive plasma ramp up scenario is introduced with plasma break down of 35 V·0.3 sec.

When total lifetime fluence restrains to 0.3 MWYr/m^2, the shield thickness is determined by criteria for nuclear heating rate (3 mW/cc) or total nuclear heating (35 kW). In a case of 3 MWYr/m^2, dose for a organic insulator becomes decisive criteria (3×10^9 rad). It requires additional shield thickness and cost. However, a large amount of cost increase is due to additional blanket cost.

Introducing the new FER magnet design conditions for TFC, winding pack averaged current density can be achieved to 43 A/mm^2 at the peak field of 12 T. Following the same design conditions for magnets, optimum magnetic field of TFC for both R-minimum and cost minimum may exist between 11 T and 12 T. Relative cost will increase slightly with decreasing magnetic field because the plasma size enlarges. On the other hand, cost sensitivity for higher field design is more sensitive

than that for lower field design. That's because not only increase of magnet cost but also increase of shield thickness and cooling cost due to high fusion power density in the case of high field coil design. If the plasma minor radius is kept constant as 1.25 m with increasing the magnetic field, some ignition margin can be expeted to plasmas. In a case of 16 T, ignition margin of 1.9 is obtained. However, the relative cost of FER would increase to about 140%. Cost efective conditions for the magnet design will exist between 11 T and 12 T.

Several other options can be considered to be sensitive. For example, scrape-off layer thickness, field ripple etc. However the ranges of these options are rather small so that total impact due to them will be small. These options are excluded from these analysis.

Table 4.12 Design assumptions and conditions for FER

Confinement scaling	$0.155\ a\ I_p\ \sqrt{\kappa}$
Beta scaling	$G\ I_p/a\ B_T$, $G = 3.5$
Safety factor	$q\psi^* = 2.6$
Plasma shape	$\tilde{\kappa} = 1.7\ /\ \tilde{\delta} = 0.2$, SND
Ignition margin	1.0
Plasma temperature	12 kev
Z_{eff}	1.48
β/β_{DT}	1.23
Maximum field of TFC	12T
Conductor occupation factor	0.65
Correction coef. of B_{Tmax}/B_{max}	1.2
Ripple at outer plasma edge	0.75 %
Free space between TFC and V.V in vertical-build	0.6 m
Number of TFC	12
Yield strength of TFC case	765 MPa
Shield attenuation in SC	0.1326
Effective shield thickness	0.81 m
Biological shield requirement	5 m rem.
Max. hot spot temp. of SC	100 K
Temperature margin of SC	2 K
Bulk temperature	4.2 K
Allowable strain of winding	8×10^{-3}
Voild area fraction	0.4
Quench voltage	10 KV
Peak field of Solenoid coils	10 T
Volt sec supplied by OHC	62.5 v.s.
Plasma breack down	10 v•1 sec
Plasma current ramp-up time	80 sec
Ignition approach time	20 sec
Plasma burn time	~ 800 sec

Table 4.13 Sensitivity of selected parameters on plasma major radius and cost

Palameters	value	R_p(m)	cost(%)	dc/dR(%/m)
Ignition margin, I_g	1.0	4.42	100.0	
	1.5	4.65	110.1	43.9
	2.0	4.84	121.3	58.9
Troyon coeff., G	3.5	4.42	100.0	
	2.8	4.54	103.1	25.8
Safety factor, q_ψ	2.6	4.42	100.0	
	3.0	4.58	103.2	20.0
	3.5	4.72	107.5	30.7
Elongation, κ	1.5	4.63	103.2	
	1.7	4.42	100.0	15.2
	2.0	4.23	100.8	-4.2
Averaged Z_{eff}	1.48	4.42	100.0	
	1.85	4.54	107.1	59.2
	2.0	4.58	109.8	67.5
Available volt-sec	65.0	4.29	98.6	
	82.0	4.42	100.0	10.8
	160.0	4.92	111.1	22.2
Fluence (MW Yr/m^2)	0.3	4.42	100.0	
	3.0	4.68	102.6	10.0
+ blanket	3.0	4.68	107.5	28.8
Peak field of TFC	8.0	4.62	105.0	
(T)	10.0	4.39	99.4	24.3
	12.0	4.37	99.3	5.0
	14.0	4.46	105.3	31.6
	16.0	4.80	120.1	43.5

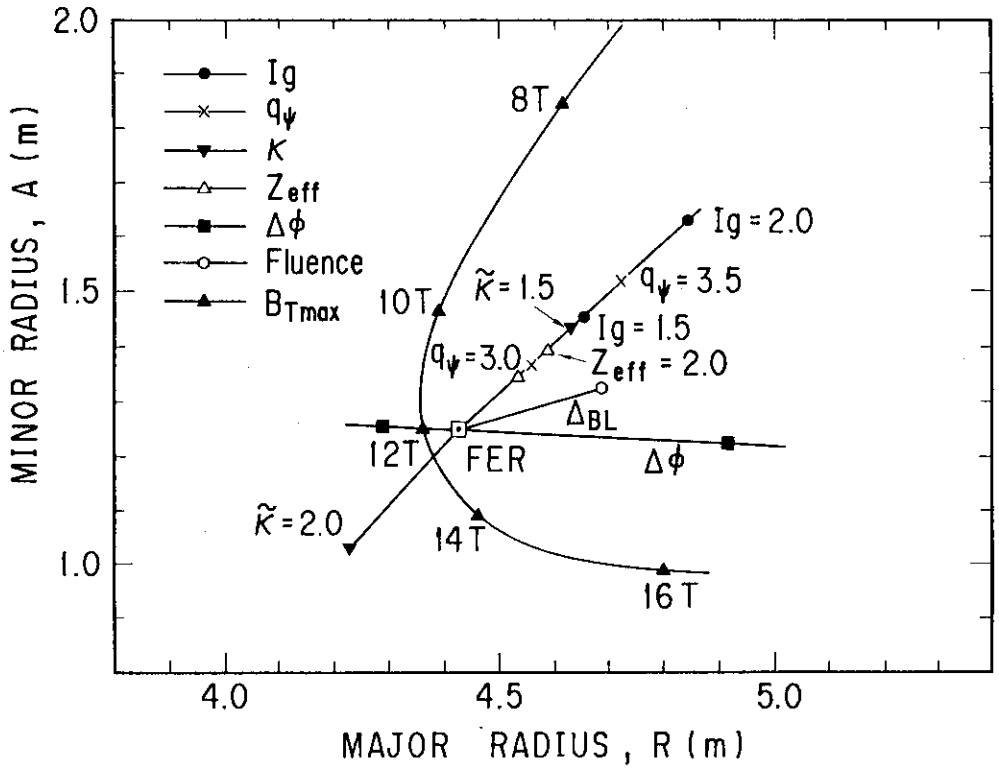

Fig. 4.4 Relations between plasma size and single parameter changes of specific design values on the basis of FER design

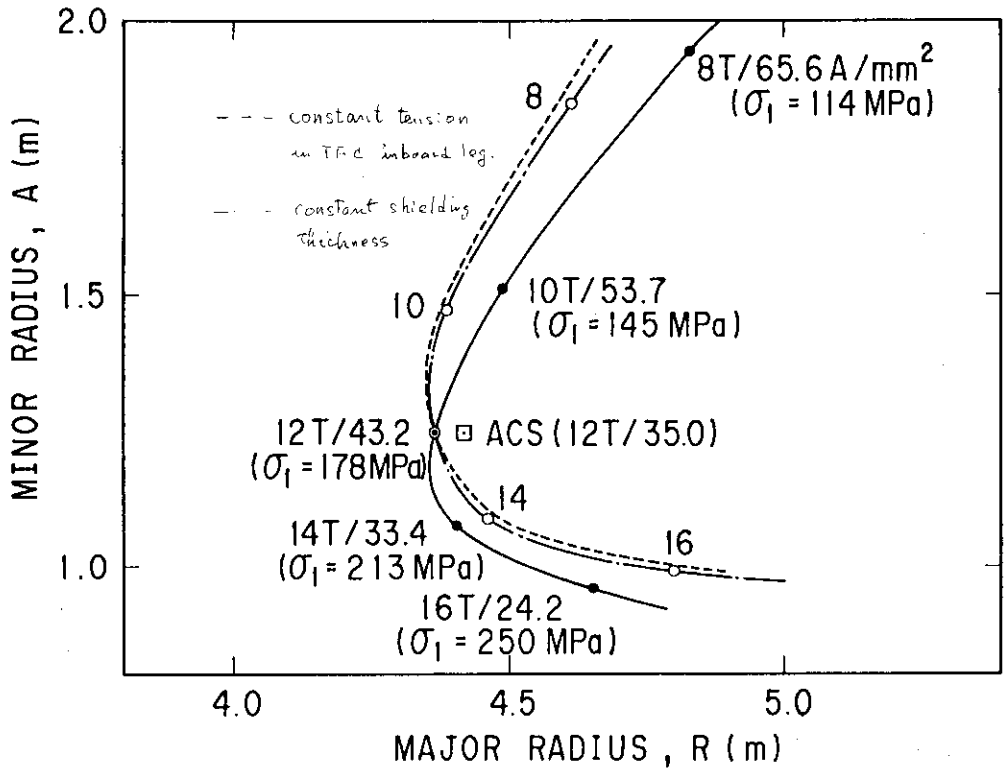

Fig. 4.5(a) Relations between plasma size and peak field constraint of TFC conductor on a-R diagram

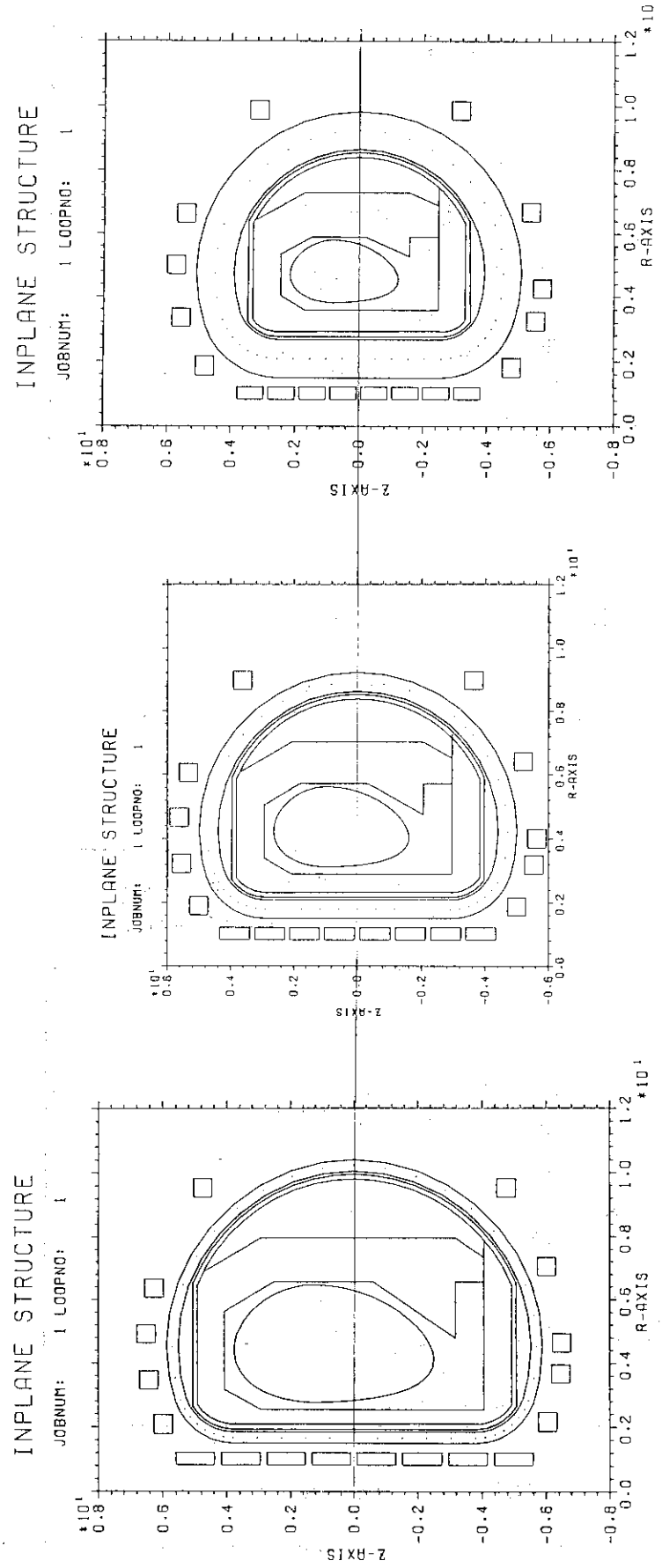

Fig. 4.5(b) Cross sections of tokamak core structures in case of different peak field constraint of TFC,
left : $B_{Tmax} = 8T$, middle : $B_{Tmax} = 12T$, right : $B_{Tmax} = 16T$.

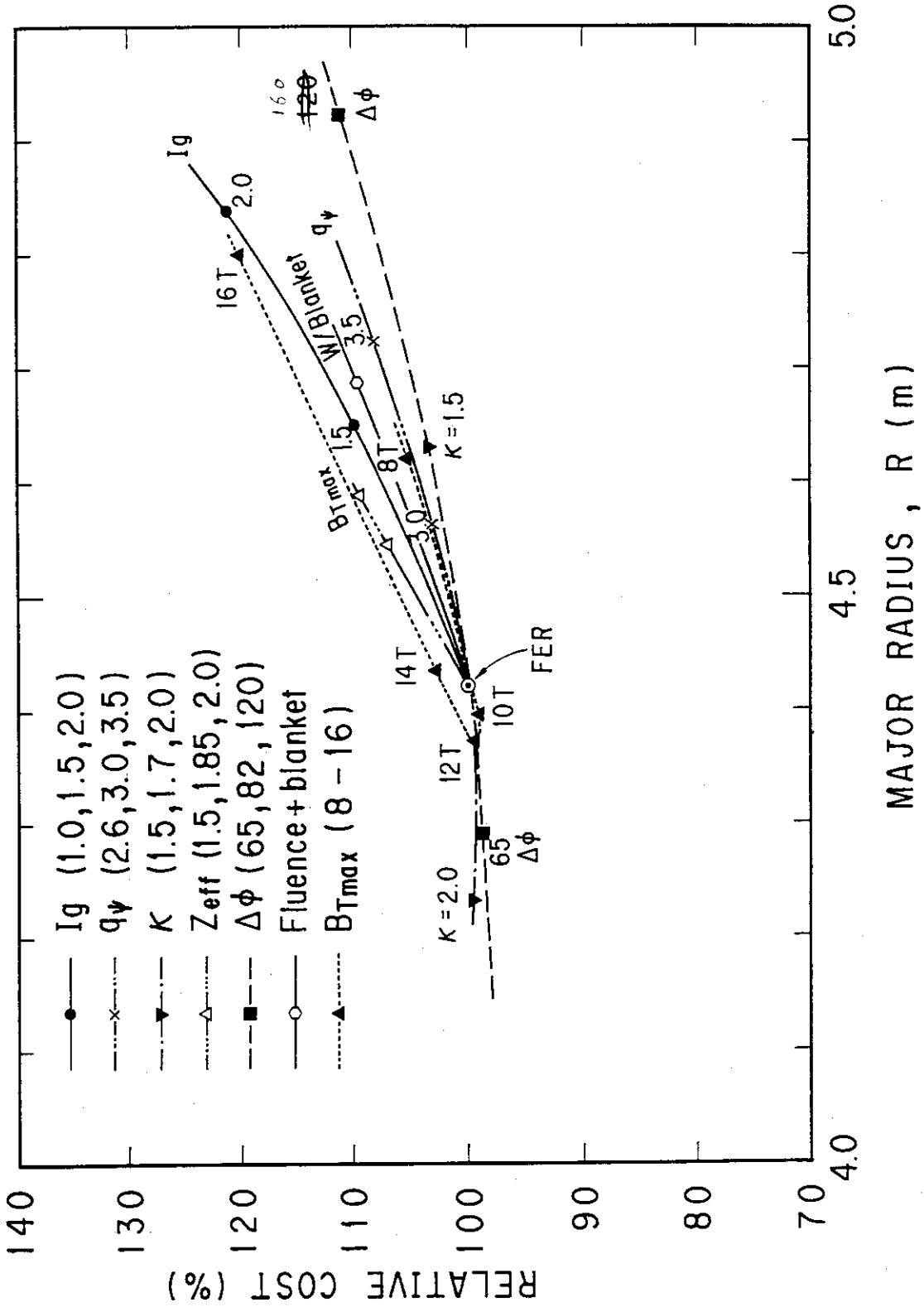

Fig. 4.6 Impact of single parameter changes on major radius and relative cost

4.4 Observations

The results of the both of global and individual sensitivity studies are summarized as follows:

For the global sensitivity studies

(1) INTOR plasma physics design
There is little impact on the INTOR design by substituting FER Physics.

(2) PFC design constraints in INTOR Engineering is rather conservative than FER.

(3) The preliminary result of cost estimations reveals that the cost of INTOR device is about 16% higher than that of the FER device.

(4) Plasma parameter sets of the both NET and FER machines give almost same ignition margin when the same Mirnov type scaling law and FER Power balance equation is used. However, some physics constraints, for example ion composition, safety factor etc., are assumed more conservatively in NET design. If FER physics assumptions and constraints are introduced in NET design, plasma major radius decreases by about 60 cm, and cost ~11%.

(5) Substitution of NET engineering constraints with those of FER, almost gives no effect on the thickness of TF coil and shield/blanket, then plasma major radius. The difference of allowable TF ripple values (FER: ±0.75%, NET: ±1.2%) gives different TF coil bore (~15 cm). However, the cost difference can be expected to be not so large.

(6) Compactness and cost reduction of the devices will be carried out mainly by choices of some design features such as (1) high noncircularity (2) hybrid operation scenario (3) thinner shield thickness associated to lower life time fluence.

For individual sensitivity studies

(1) With few exception the changes which increase plasma major radius generally leads to capital cost increase.

(2) The changes which leads to the major radius (R_p) change are divided into the following three groups by the intensity of impact on the capital cost ($\frac{d}{dRp}$).

Strong impact group:

B_t larger than 12 T, Ignition margin, Z_{eff}

Medium impact group:

Shield thickness, safety factor, elongation smaller than 1.7, B_t smaller than 10 T, $\Delta\phi$ larger than 50 v.s.

Week or no impact group:

elongation larger than 1.7, $\Delta\phi$ smaller than 50 v.s.

5. Relative cost comparison

Relative cost estimations are carried out for five INTOR-like devices. Fig.5.1 shows the comparative pictures of the reactor core structures for five machines. Itemized direct capital cost breakdown relative to FER/ACS is shown in Fig.5.2. The total construction costs of INTOR, NET, TIBER, and OTR relative to FER are 116%, 127%, 82%, and 160% respectively. Fraction of direct cost for each device is shown in Table 5.1. It is shown in Fig. 5.3 that the relative cost is smoothly correlate to the plasma major radius. Some remarks for the above results are following :

(1) Basically, the relative cost of five INTOP-like devices appears on a smooth correlation with reactor size. Deviation from the smooth function seems to be different choices of design features/drivers.
(2) FER and TIBER have no tritium breeding blanket. That means a direct cost reduction of that amount.
(3) FER and TIBER chose non-inductive current ramp-up. Other three, INTOR, NET, and OTR choose full inductive current ramp-up as reference operation scenario. Latter operation scenario gives a great impact on electric power supply system.
(4) The reference of current drive and heating systems in FER is LHCD and ICRH respectively. However, LH system is designed to be capable for plasma heating also. In ignition approach phase, both powers of LHH and ICRH are injected for plasma heating. If LHCD and ICRH systems are installed individually, additional cost for heating system is required.
(5) IN TIBER, the cost of NBI system is not included. On the other hand, LHCD system is included in the initial capital cost of INTOR.
(6) For a large machine such as OTR, the cost of magnet systems, especially TF coils, becomes a dominant element. It is, on the other hand, greatly saved for smaller machine such as TIBER.

Table 5.1 Relative costs of intor-like devices evaluated by trescode

COST	INTOR	NET	FER	TIBER	OTR
Total Construction Cost (%)					
I. Relative to FER	116	127	100	82	160
II. Relative to INTOR	100	109	86	71	138
Fraction of Direct Cost (%)					
1. Torus structure	14.2	17.4	15.2	13.3	17.9
2. Blankets or test module	2.8	4.2	0.4	0.5	3.9
3. TFC and other magnets	17.7	17.0	16.3	12.7	21.3
4. PFC magnets	6.7	6.7	9.0	6.9	8.3
5. Heating and/or CD systems	14.0	11.5	16.0	20.4	11.1
6. Electrical power systems	11.2	10.6	7.0	7.9	8.5
7. Sub systems (Fuel, Vacuum, etc)	7.1	7.1	7.0	7.2	5.9
8. Cooling (Liq. He, Liq. N, H_2O)	5.7	4.8	6.0	6.3	3.3
9. Diagnostics & control system	5.2	4.7	6.0	7.3	3.8
10. Reactor assembling	7.5	8.7	8.1	7.1	10.0
11. Building facilities	7.9	7.3	9.0	10.4	6.0

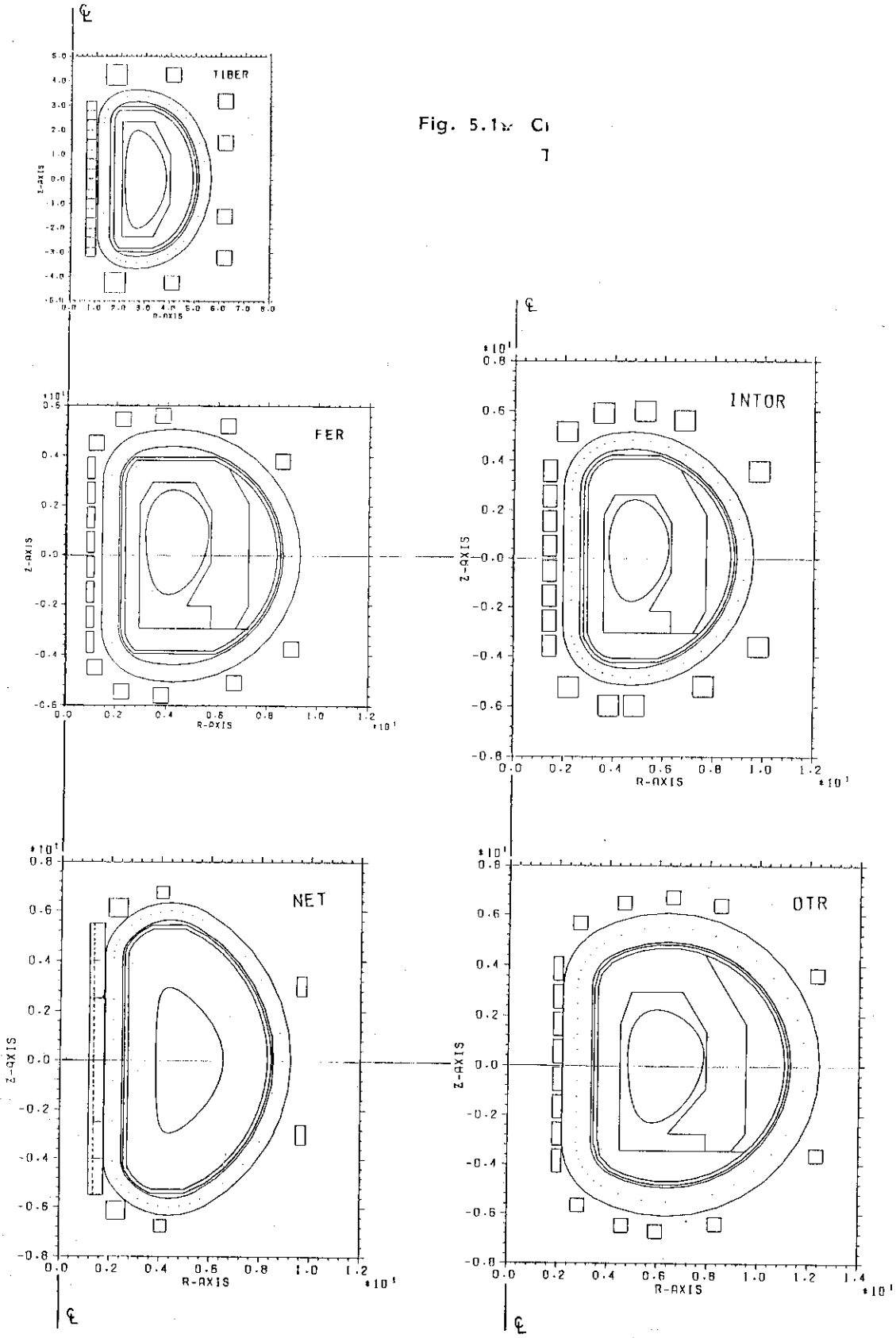

Fig. 5.1 Cross sections of tokamak core structures of INTOR-like designs; TIBER, FER, INTOR, NET and OTR.

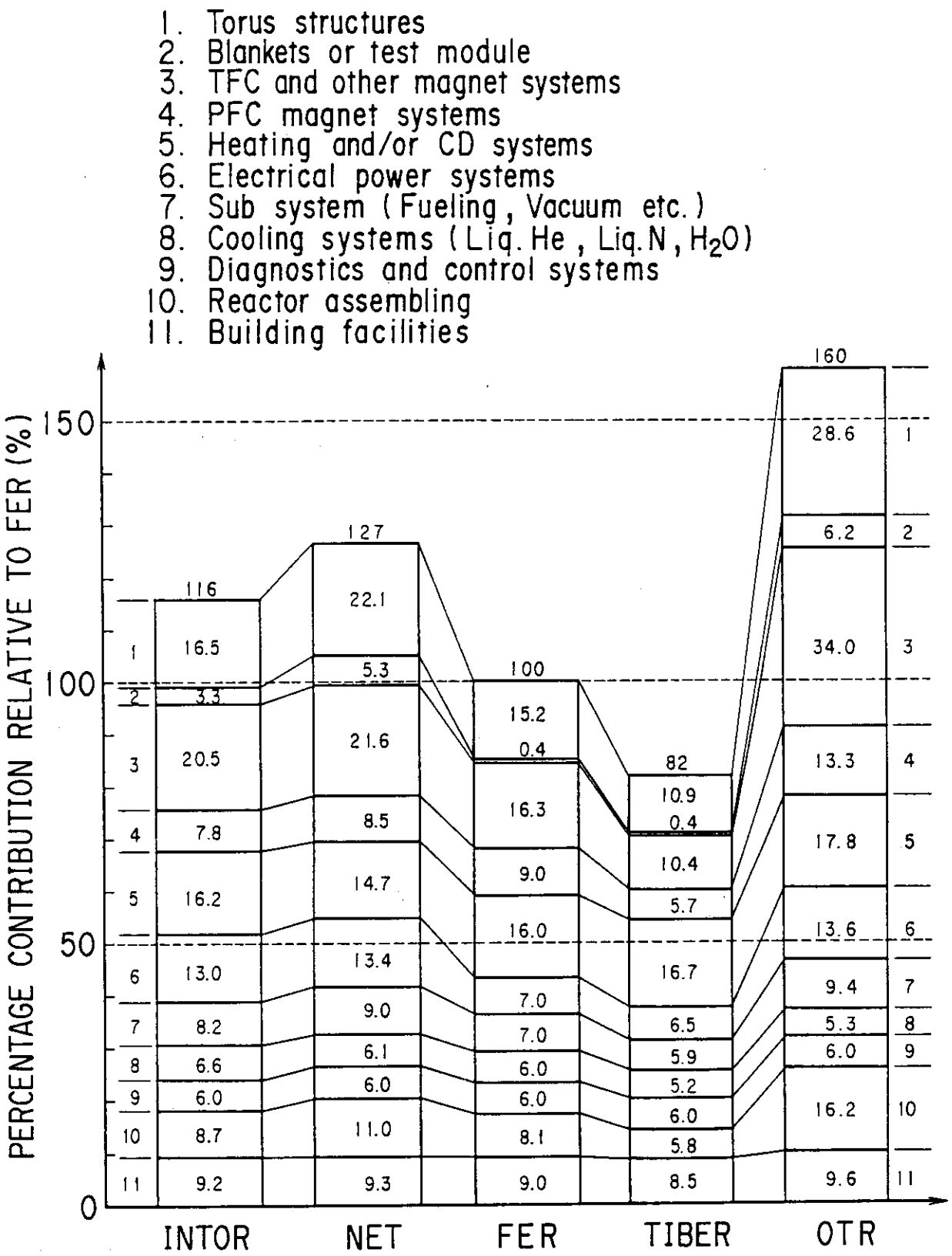

Fig. 5.2 Itemised direct capital cost breakdown relative to FER evaluated by trescode

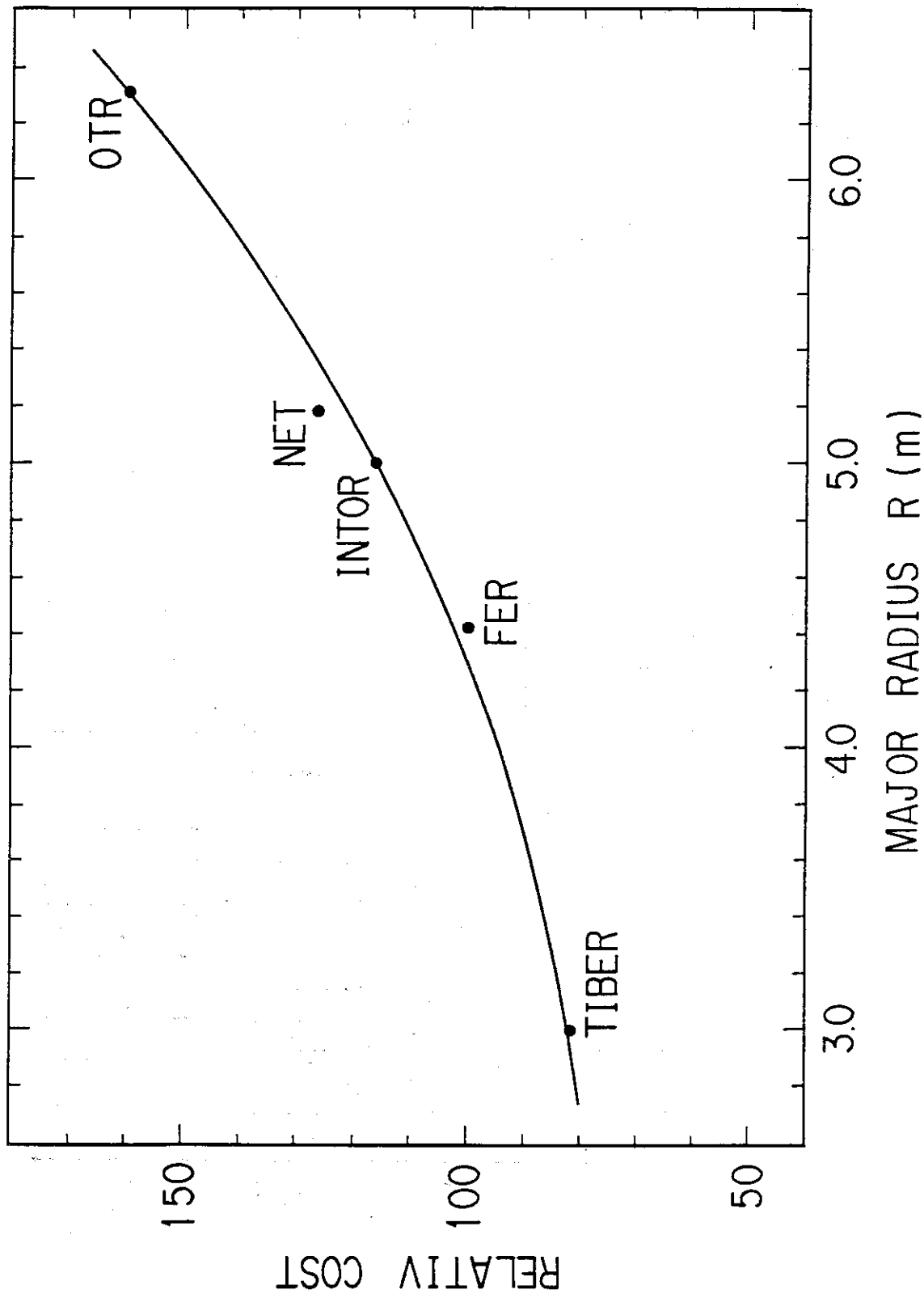

Fig. 5.3 Relative cost of five INTOR-like designs as a function of major radius

Acknowledgement

The authors are grateful to Drs. S. Tamura, M. Yoshikawa, K. Tomabechi and S. Mori for their continuing encouragement.

References

(1) T. Mizoguchi, M. Sugihara, K. Shinya et al., Development of Tokamak Reactor Conceptual Design Code "TRESCODE" - Conceptual Design Study of FY86 FER-, Japan Atomic Energy Research Institute Report, JAERI-M 87-120 (1987).

(2) Report of IAEA INTOR-related Specialists' Meeting on Engineering Test Reactor National Design Concepts (March 1987)

Acknowledgement

The authors are grateful to Drs. S. Tamura, M. Yoshikawa, K. Tomabechi and S. Mori for their continuing encouragement.

References

(1) T. Mizoguchi, M. Sugihara, K. Shinya et al., Development of Tokamak Reactor Conceptual Design Code "TRESCODE" - Conceptual Design Study of FY86 FER-, Japan Atomic Energy Research Institute Report, JAERI-M 87-120 (1987).

(2) Report of IAEA INTOR-related Specialists' Meeting on Engineering Test Reactor National Design Concepts (March 1987)